MOLECULAR AND CELLULAR BIOLOGY, May 1996, p. 2431–2444 Vol. 16, No. 5
0270-7306/96/$04.00+0

Multiple Roles of the Novel Protein Tyrosine Phosphatase PTP3 during *Dictyostelium* Growth and Development

MARIANNE GAMPER,[1] PETER K. HOWARD,[1,2] TONY HUNTER,[2] AND RICHARD A. FIRTEL[1]*

Department of Biology, Center for Molecular Genetics, University of California, San Diego, La Jolla, California 92093-0634,[1] and Molecular Biology and Virology Laboratory, The Salk Institute for Biological Sciences, San Diego, California 92186-5800[2]

Received 10 October 1995/Returned for modification 6 December 1995/Accepted 16 February 1996

PTP3, the third nonreceptor protein tyrosine phosphatase identified in *Dictyostelium discoideum*, has a single catalytic protein tyrosine phosphatase domain. Recombinant PTP3 exhibited phosphatase activity that was inhibited by vanadate. *PTP3* is expressed at a moderate level during growth. The level of transcripts increased between growth and 8 h of development and declined thereafter. Expression of *lacZ* under the control of the *PTP3* promoter indicated a spatial localization of PTP3 in the anterior-like and prestalk cell types. There are two copies of the *PTP3* gene in this haploid organism. Disruption of one copy led to a slow-growth phenotype. We were unable to obtain a strain with disruptions in both *PTP3* genes. Overexpression of wild-type PTP3 led to slower growth rates and the formation of large aggregation streams. These streams split into smaller aggregates, many of which then arrested in development. Overexpression of a catalytically inactive mutation (Cys to Ser) had no effect on growth rate; however, this strain also formed large aggregation streams that later split up into large and small mound structures and became fruiting bodies of various sizes. Antiphosphotyrosine Western blot (immunoblot) analysis of total cell proteins showed that the pattern of protein tyrosine phosphorylation was specifically altered in PTP3 mutants. Addition of growth medium to starving cells and a subsequent replacement with nonnutrient buffer led to reciprocal changes in the pattern of several phosphotyrosine proteins, including a protein of ~130 kDa. Analysis of strains overexpressing active or inactive PTP3 suggested that p130 is a potential substrate of PTP3. A transient posttranslational phosphorylation of PTP3 further supported the role of PTP3 in these processes. The data obtained strongly suggest new regulatory functions for PTP3 that are distinct from those described earlier for *D. discoideum* PTP1 and PTP2.

Dictyostelium discoideum grows as single-celled amoebae, but upon starvation, it initiates a developmental process that leads to the formation of a multicellular structure consisting of spore and stalk cells. This relative simplicity has made *D. discoideum* a model system for studying eukaryotic signal transduction and cell-cell communication (for a review, see references 10, 16, and 63). Several hours after starvation, *D. discoideum* amoebae aggregate in response to nanomolar pulses of the chemoattractant cyclic AMP (cAMP). By 9 h, 10^3 to 10^5 cells form a mound. A rise in the cAMP concentration to micromolar levels occurs (1), which initiates a developmental cascade through the activation of the transcription factor G-box-binding factor (45, 46). This results in the initiation of cell-type-specific gene expression, tip formation, and the sorting out of prestalk cells. Subsequently, in the migrating slug, prestalk cells are localized to the anterior ~15% of the organism, prespore cells are found in the posterior, and the anterior-like cells (ALCs) are scattered throughout. During culmination, prestalk cells penetrate through the prespore-cell mass and lift it off the substratum. Finally, the cells mature into spore and stalk cells and form the final structure with a sorus atop a slender stalk.

Schweiger et al. (47) first reported evidence for phosphotyrosine (pTyr)-containing proteins in vegetative cells of *D. discoideum* and speculated about the involvement of protein tyrosine kinases and protein tyrosine phosphatases (PTPs) in regulating developmental processes. Two developmentally regulated *D. discoideum* protein tyrosine kinases have been reported to date (58), but the importance and diversity of protein tyrosine phosphorylation in this organism suggest that one can expect additional protein tyrosine kinases to be identified.

We have identified three nontransmembrane PTPs (for a review, see reference 17). PTP1 and PTP2 are both developmentally regulated and expressed later in development in a pattern similar to that of ALCs (27, 28). Gene disruptions of either of these PTPs resulted in only minor effects on growth and development. *ptp1*-null cells showed an accelerated developmental timing, whereas *ptp2*-null cells formed larger structures than did the wild type (wt) if plated at low cell densities. Growth rates and developmental morphologies were indistinguishable from those of wt cells. Despite these similarities, the analysis of overexpression phenotypes and the pattern of pTyr-containing proteins in null and overexpressor strains suggested specific roles for the two PTPs. Strains overexpressing PTP1 to a high level fail to aggregate, and moderate overexpressors form aggregates with multiple tips and very aberrant slugs and final structures (28). Strains overexpressing PTP2 to a high level develop to the mound stage and arrest for 6 to 8 h (27). A variable fraction of the aggregates then proceed with development and form small fruiting bodies. Overexpression of either PTP led to lower growth rates. Immunostaining of blots of total cell proteins from PTP1 and PTP2 mutant strains with anti-pTyr antibodies gave discrete patterns of pTyr-containing proteins that were different from those of wt cells and from each other. Moving cells starved for 4 h from nonnutrient buffer to growth medium led to cell rounding, which was accompanied by major changes in the pTyr protein pattern. Analyses of disruption mutants and overexpressing strains have shown that PTP1 but not PTP2 is involved in this process,

* Corresponding author. Mailing address: Center for Molecular Genetics, Rm. 225, University of California, San Diego, 9500 Gilman Dr., La Jolla, CA 92093-0634. Phone: (619) 534-2788. Fax: (619) 534-7073.

TABLE 1. Comparison of mutant PTP phenotypes

Strain	Growth characteristic(s)	Development characteristic(s)	pTyr protein pattern[a]:	
			During development	After medium shift
KAx-3 (wt)	wt	wt	Increase in pTyr of 97- and 55-kDa proteins at 10 h; pTyr levels remain high in late development	Increase in pTyr in p130 and p43 (actin) after shift from buffer to medium; decrease after shift to buffer
ptp1 null[b]	Small cells; wt growth rate	Accelerated; wt structures	p97 pTyr same as in wt; constitutive, high levels of p55 pTyr	p130 same as in wt; prolonged pTyr in actin after shift to buffer
ptp2 null[b]	Cell size and growth rate same as wt	Larger structures than wt	Constitutive, high levels of pTyr in p97 and p55	No effect on pTyr in p130 or actin
ptp3 null	Not existent			
ptp3 partial knockout	Large cells; lower growth rate	Normal development	Elevated pTyr levels in p97 and p55 between 10 and 20 h	No effect on pTyr in p130 or actin
PTP1 overexpressor[b]	Cell size same as wt; reduced growth rate	Strong overexpressors: Agg^-; moderate overexpressors: morphological abnormalities	Constitutive, low levels of pTyr in p97 and p55	p130 same as in wt; lower pTyr levels in actin and faster dephosphorylation
PTP2 overexpressor[b]	Small cells; low growth rate	Arrest at mound stage for 6 to 8 h	Constitutive, low levels of pTyr in p55; increase in p97 pTyr at 16 h	No effect on pTyr in p130 or actin
PTP3 (wt) overexpressor	Cell size same as wt; lower growth rate	Large aggregation streams; partial arrest at mound stage	Smaller increase in pTyr level of p97 and p55; delayed phosphorylation of p97	Strongly reduced p130 phosphorylation rate; actin same as in wt
PTP3 S649 overexpressor	Small cells; growth rate same as wt	Large aggregation streams; large structures	Elevated pTyr levels in p97 and p55 between 10 and 20 h	Prolonged pTyr in p130 after the shift to buffer; actin same as in wt

[a] Only pTyr proteins relevant for the changes in PTP3 mutants are described.
[b] Data from reference 27 to 29.

and PTP1 was found to differentially affect the cell shape change and actin tyrosine phosphorylation (29). The phenotypes of PTP1 and PTP2 mutants are summarized in Table 1.

In this report, we describe the characterization of PTP3, the third PTP isolated from *D. discoideum. PTP3*, as was found for *PTP1* and *PTP2*, is preferentially expressed in prestalk cells and ALCs during development. Two copies of the *PTP3* gene exist in *D. discoideum*. Several gene disruption approaches were used, but we were only able to disrupt one gene. Overexpression of wt and mutant forms of PTP3, including a catalytically inactive form, suggests that PTP3 plays a role during aggregation and at the mound stage at the transition between aggregation and multicellular differentiation. Growth medium shift experiments (see above) with mutant PTP3 strains identified a 130-kDa pTyr-containing protein (pp130) as a potential PTP3 substrate. The medium shift resulted in a transient posttranslational phosphorylation of PTP3, identified as reduced mobility on polyacrylamide gels that was affected by pretreatment of the samples with protein phosphatase 2A (PP2A). Our data suggest that during growth and development, PTP3 has very specific roles that are distinct from those of PTP1 and PTP2.

MATERIALS AND METHODS

PCR amplification of *D. discoideum* DNA and screening of cDNA and chromosomal libraries. The reaction conditions and degenerate oligonucleotides used to amplify genomic DNA derived from the axenic strain KAx-3 were as previously described (27). Sequence analysis of an ~500-bp fragment obtained with primers 2 and 3 (see Fig. 2) revealed a novel PTP, termed PTP3. This PCR fragment was used to screen a 12- to 16-h developmental λ-ZAP cDNA library (46), and a cDNA clone (clone 17) of ~3.3 kb which contained the entire PTP3 open reading frame was isolated. Screening of a genomic *Sau*3A library (13) with an ~500-bp 5′ cDNA probe identified plasmid pMG1. Restriction digestion analysis and transformation of a version of this plasmid encoding G418 resistance (pMG14, see below) into *D. discoideum* followed by Northern (RNA) and Western blot (immunoblot) analysis showed that the 6.1-kb genomic insert of pMG1 contained the whole *PTP3* promoter, coding sequence, and transcription termination region.

Plasmid constructions. Standard molecular biological techniques were used as described in reference 43. Most plasmids described in this report are shown in Fig. 1B. All plasmids used for overexpressing PTP3 in *D. discoideum* were based on plasmid pMG1 with the pAT153L backbone (22). For overexpression of wt PTP3, a 2.2-kb fragment with a neomycin resistance gene ($G418^R$) under the control of the *D. discoideum actin6* promoter (40) was cloned into the *Asp*718 site localized 3′ to the PTP3 coding region. The Cys (TGT)-to-Ser (AGT) mutation (S649) was introduced by PCR amplification of the ~500-bp *Eco*RV-*Pst*I cDNA fragment cloned into pBluescript SK− (Stratagene) with the T7 primer and an oligonucleotide carrying the point mutation and the *Pst*I site (5′-CAAAAACT GCAGAACTGTGGACTATAACT-3′). Subsequently, the ~100-bp *Hae*III-*Pst*I fragment of pMG14 was replaced by the same fragment containing the S649 mutation, giving plasmid pMG33. Plasmid PTP3Δ1 S649 contains a deletion of ~350 bp created in pMG33 by fusing the 5′ *Nsi*I site to the *Ssp*I site. Plasmid PTP3Δ2 contains an ~700-bp deletion between *Hae*III and *Bgl*II, including part of the catalytic region. To obtain these in-frame deletions, some linker nucleotides had to be added. All fusion sites and the entire PCR fragment carrying the S649 mutation were verified by sequencing.

For the PTP3–β-galactosidase (β-Gal) reporter plasmid pMG22, the *PTP3* promoter and the first two amino acids of the PTP3 coding sequence were fused in frame to the ninth codon of *lacZ* by exchanging the *SP60* promoter of plasmid *SP60-lacZ* (22) with the 1.8-kb *Xba*I (in the multiple-cloning site)-*Eco*RV fragment of pMG1. The construction of pMG22 was done in three cloning steps, and the correct fusion was verified by restriction digestion analysis.

Construction of the gene disruption plasmid pMG5 was accomplished in two steps: first, by cloning the genomic *Hin*cII-*Xba*I fragment (~3.0 kb) of pMG1 into pBluescript SK−, giving plasmid pMG3, and second, by replacing the ~600-bp *Eco*RV-*Pst*I fragment (part of the catalytic domain) with the 3.2-kb fragment containing the *THY1* gene (13). A second *PTP3* disruption plasmid was made by replacing the ~700-bp *Hae*III-*Bgl*II fragment of pMG3, including part of the catalytic domain, with a 1.3-kb fragment carrying the blasticidin S resistance gene (*bsr*) flanked by the *actin15* promoter and the *actin8* terminator (57) (for the localization of restriction sites, see Fig. 1).

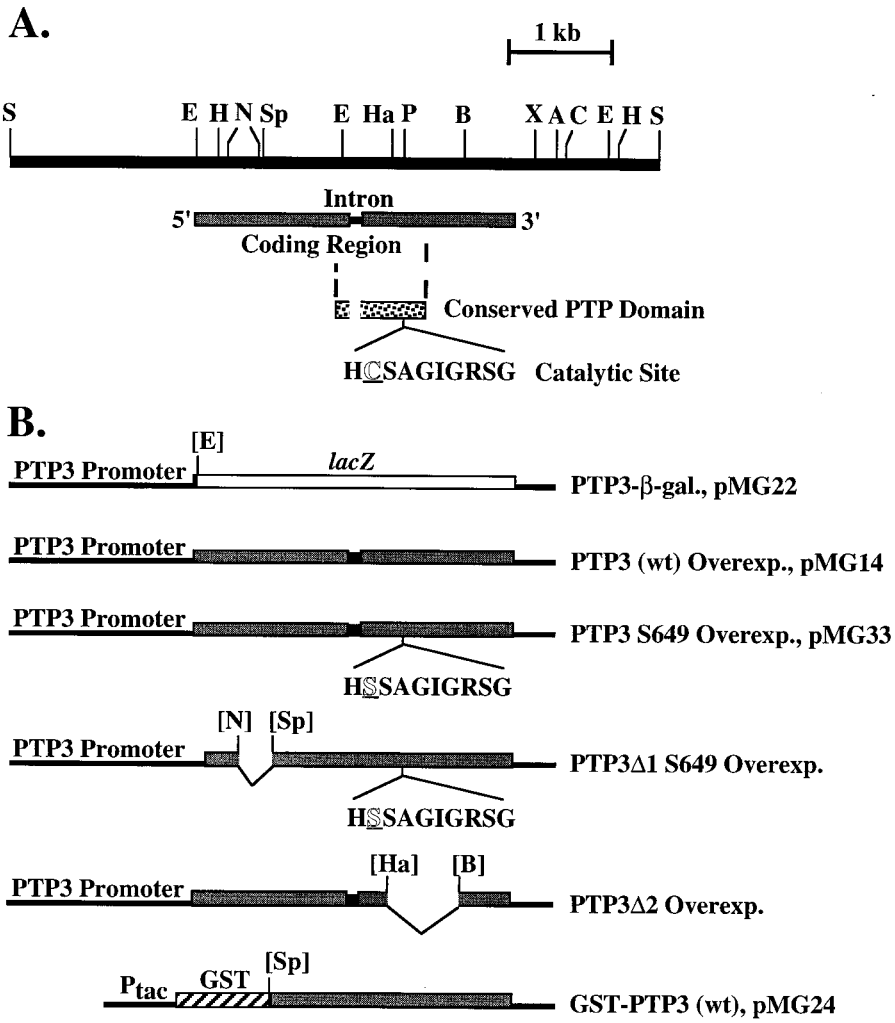

FIG. 1. Maps of *PTP3* genomic DNA and plasmid constructs. (A) The restriction analysis data are derived from genomic Southern blots and the mapping of genomic clone pMG1. The 6.1-kb fragment shown corresponds to the insert in pMG1. All sites for *Eco*RV (E), *Hin*cII (H), *Nsi*I (N), *Pst*I (P), *Bgl*II (B), *Xba*I (X), *Asp*718 (A), and *Cla*I (C) are shown. Only the *Sau*3A (S), *Ssp*I (Sp), and *Hae*III (Ha) sites which were relevant during this study are indicated. The locations of the only known intron, the coding region, the catalytic PTP domain, and the conserved site directly involved in dephosphorylation are also shown. (B) Maps of plasmid constructs. The *PTP3* promoter, located in the 1.8-kb untranslated upstream region, controls the expression of wt and mutant *PTP3* as well as *PTP3-lacZ*. Overexpression (Overexp.) was achieved by multiple insertions of these constructs into the *D. discoideum* genome. The in-frame fusion sites are labeled with the restriction sites from the original sequence. Brackets indicate that they have been destroyed during subclonings.

For the expression of functional *PTP3* in *Escherichia coli*, the C-terminal 747 amino acids of PTP3 were fused to glutathione *S*-transferase (GST) by inserting the ~2.3-kb *Ssp*I-*Xho*I cDNA fragment (the *Xho*I site is located in a multiple-cloning site beyond the PTP3 coding sequence) into the pGEX-KG expression vector (20), which was cut with *Eco*RI, treated with Klenow polymerase, and cut with *Xho*I.

Culturing and development of *D. discoideum* strains, transformation into *D. discoideum*, and selection and analysis of clonal isolates. The axenic *D. discoideum* wt strain KAx-3 was used for overexpression studies. The gene disruption construct pMG5 was electroporated into the thymidine auxotrophic strain JH10, a derivative of KAx-3 (23, 37). Cells were grown in HL5 medium, supplemented with 10 to 20 μg of G418 per ml or with 100 μg of thymidine per ml, as required. Thirty micrograms of linear plasmid DNA was used per electroporation. For the maintenance of a high level of overexpression, continuous selection for $G418^R$ was required as previously described (27). Clonal populations of cells were isolated as described previously (23, 27). The level of overexpression was assayed by β-Gal staining (28) or Northern blot (36) or Western blot analysis (see below). Potential gene knockout strains were analyzed by Southern blot analysis (43). Growth phenotypes were investigated in shaking cultures or on a *Klebsiella aerogenes* lawn (27), and developmental phenotypes were monitored by plating starved cells on nonnutrient sodium-potassium phosphate plates (23).

***lacZ* reporter strains and β-Gal staining.** The experiments were performed as previously described (27, 28).

Expression and isolation of GST-PTP3 and measurement of PTP activity. *E. coli* BL21(DE3) (43) carrying the GST-PTP3 expression plasmid was grown in 1 liter of "terrific" broth (43) at room temperature for ~10 h. Then, IPTG (isopropyl-β-D-thiogalactopyranoside) at a final concentration of 0.1 mM was added and the culture was incubated for another 12 h. The fusion protein was purified by glutathione-agarose affinity chromatography (50). Cells were harvested by centrifugation and washed in 0.1 M Tris (pH 8.0)–25 mM EDTA (pH 8.0)–5% glucose. The cell pellet was resuspended manually with a spatula in 10 ml of phosphate-buffered saline (PBS) (43)–5 mM EDTA, pH 8.0. One milliliter of lysozyme (50 mg/ml) was added, the suspension was mixed, and the cells were incubated on ice for 20 min. Fifteen milliliters of lysis buffer [10 mM EDTA (pH 8.0), 1 mM ethylene glycol-bis(β-aminoethylether)-N,*N*,*N*′,*N*′-tetraacetic acid (EGTA) (pH 8.0), 3 mM dithiothreitol, 1 mM phenylmethylsulfonyl fluoride, and aprotinin (40 μg/ml) in 1× PBS] and Triton X-100 (final concentration, 1%) were added. After sonication and removal of cell debris by centrifugation, the supernatant was incubated with ~2 ml of glutathione-Sepharose 4B beads (Pharmacia) for 1 h at 4°C with gentle rocking. The beads were then washed with lysis buffer (including Triton X-100) and PBS–1 mM dithiothreitol, and the fusion protein was eluted with 5 ml of 10 mM glutathione (in 50 mM Tris, pH 8.0). Fractions of 400 μl were collected and subsequently analyzed on a sodium dodecyl sulfate (SDS)-polyacrylamide gel.

The PTP activity of the isolated fusion protein was tested with *para*-nitrophenyl phosphate (*p*NPP) as a substrate, and the assay conditions were similar to

those previously reported (28). PTP activity was assayed at room temperature in a 1-ml volume containing 50 mM imidazole (pH 7.5), 0.1% β-mercaptoethanol, 20 mM *p*NPP, and an estimated 1 or 2 μg of GST-PTP3 per assay. When indicated, sodium orthovanadate (Na_3VO_4) was added at a final concentration of 2 μM. Six parallel reactions were run for 116 min on a Perkin-Elmer UV spectrophotometer and the A_{410} was measured every minute for each sample. The molar absorptivity (ε) of $1.78 \times 10^4\ M^{-1}\ cm^{-1}$ (59) was used to calculate the concentration of *p*-nitrophenolate ion produced in the reaction. pTyr phosphatase activity was assayed as described by Streuli et al. (53).

Antibodies and Western blot analysis. The GST-PTP3 fusion protein (see Fig. 1) was injected into rabbits to raise polyclonal anti-PTP3 antibodies. After the serum was passed through a column of immobilized GST, the PTP3-specific antibodies were purified by their cross-reaction with the GST-PTP3 fusion protein immobilized on glutathione-Sepharose 4B beads. GST and the GST fusion protein were immobilized by cross-linking with dimethylpimelimidate as described for the method of covalently attaching antibodies to protein A beads (26). Serum purification was performed as described previously (26). The monoclonal anti-pTyr antibody py72 was used for anti-pTyr Western blotting (19).

Total protein samples for studying changes during development or growth shifts were collected as described previously (27). SDS-polyacrylamide gels (6, 8, or 10% polyacrylamide) were run, and the size-fractionated proteins were transferred to Immobilon-P membranes (Millipore) using a Bio-Rad semidry transfer system (with Bjerrum transfer buffer used according to the manufacturer's instructions; transfer conditions, 30 min, 13 V, 4°C) or the Hoechst wet transfer system (Mighty Small Transphor Tank Transfer Unit; transfer buffer, 43.5 g of glycine, 9 g of Tris-Base, 3 g of SDS, and 600 ml of methanol in a total volume of 3 liters; transfer conditions, 90 min, 60 V, 4°C). After blotting, the membranes were air dried and incubated directly in the primary antibody solution, according to the suggestions made by Millipore. Enhanced chemiluminescence (ECL kit; Amersham) was used for detection as recommended by the manufacturer.

Immunoprecipitation and PP2A assay. Cells (wt) overexpressing the PTP3Δ1 S649 protein (Fig. 1B) were starved in sodium-potassium phosphate buffer at a concentration of 10^7 cells per ml for 2.5 h. Then, they were resuspended in growth medium (HL5) at 5×10^6 cells per ml and incubated for another 15 min. For one immunoprecipitation, 2.0×10^7 cells were lysed on ice in 1 ml of NP-40 buffer (1× PBS [pH 7.4], 1% Nonidet P-40, 10 mM NaF, 2 mM EDTA [pH 7.2], 1 mM sodium PP_i, 0.8 μg of leupeptin per ml, and 4 μg of aprotinin per ml) for 5 to 15 min. After a 10-min centrifugation, the supernatant was incubated with purified anti-PTP3 antibody for 1 h at 4°C with gentle rocking. A total of 45 μl of 50% protein A-Sepharose (Sigma) was added, and the incubation was continued for 40 min at 4°C with gentle rocking. After being washed three times in 500 μl of NP-40 buffer, the immunoprecipitates were washed twice in PP2A buffer (50 mM Tris [pH 7.0], 1 mM EDTA [pH 7.2], 50 mM β-mercaptoethanol, 1 mM $MnCl_2$, 5 μg of aprotinin per ml, and 1 μg of leupeptin per ml [65]). The immunoprecipitates were incubated in 100 μl of PP2A buffer containing 1.1 mU of PP2A (catalytic subunit from bovine heart) for 30 min at 37°C. microcystin LR (Sigma) at a final concentration of 10 μM was used as an inhibitor. After two washing steps in 450 μl of PP2A buffer containing 5 μM microcystin LR, the immunoprecipitates were eluted from the beads by boiling in SDS sample buffer.

Nucleotide sequence accession number. The GenBank (4) nucleotide accession number for *PTP3* is U38197.

RESULTS

Isolation and sequence analysis of *PTP3*. Genomic sequences encoding part of PTP3 were identified in the same PCR screen as PTP2 (27) by using degenerate oligonucleotides against highly conserved regions in the catalytic PTP domain. Genomic DNA (pMG1) and cDNA (clone 17) clones, both carrying the entire PTP3 coding region, were isolated (see Materials and Methods). A comparative restriction enzyme digestion analysis with these two plasmids predicted an intron of ~100 bp between the second *Eco*RV site and the *Pst*I site (Fig. 1). Without a complete sequence of the genomic clone, this finding does not exclude the presence of additional introns, especially toward the 3′ end beyond the *Bgl*II site. Sequence analysis of the cDNA revealed an open reading frame of 989 amino acids with a predicted molecular weight of 110,000 (Fig. 2). The catalytic PTP3 domain of 257 amino acids was flanked by N-terminal and C-terminal domains of 459 and 273 amino acids, respectively. These flanking regions showed no homologies to other proteins in the databases. There was also no evidence of a membrane-spanning sequence, suggesting that PTP3 is a soluble protein. PTP3 has a significant number of homopolymer runs of Asn, Ser, Thr, and Gln, a feature which is not uncommon for *D. discoideum* coding sequences (6, 32, 37, 49). Very striking is the run of 50 Asn (AAT) residues between the two *Nsi*I sites (Fig. 1 and 2). Besides the total of 187 Asn residues, Ser, Thr, Gln, Leu, and Pro (153, 64, 64, 60, and 57 residues, respectively) are also highly abundant amino acids.

```
MISSSMSYRH STNSVYTLNP HLNIPISTST TIPPTSFYAN NTPEMIQSQS
ENTNTNNINN SSSNINNNNN NTPDSMSMST SLSSSPSVSF NHLDLNSINN  100
KINNNTTTNN NNNNNNNNDD KFDTNALKLS NTMIIKNNNN NNNNNNNNNN
NNNNNNNNNN NNNNNNNNNN NNNNNNNNNN NNNNNNSNSN IEINVPSIQF  200
DNEPAMEVDS VAPLNVPSNH TRTTLAMHNT KSLSTSNIGL LNILPNQQSS
SSSSLSSTTT TTTTTSSSLL MPQSLFNNST YNNHHNNNNS SNAGIVGGLN  300
GSTSSLPTQA QVQLQQMQQQ MQQHQQHQYK KANLSSLSTV VDNNLNNNPM
NTSTSSPAQP NASPFSFSSS SLFSNSSLSN SGSGSASTTS TSTSSSNSMS  400
SSPPPSLKTS FSQLDEDREK MRLEFEMIKK PEMASKKSHK HHQRHYSHND
LDNRKHDEEK FFSALQPNNY GKNRYHDVLP NESTRVRLTP IESGDGDYIN  500
ANYINGEVPN SYRYYIACQA PLPSTIKDFW RMVWEERSSV IVCLTKLEEN
GKKKADVYYP ETSQAQEYGS FWIHLHKKVM FKDIGVSSLH LYKKGEEFPR  600
EVVLLHYTQW PDCGAPPSSS HIRTLSVMVN TFKARGSAKN TNGPVIVHCS
AGIGRSGTFI SININMAKIE RFGNDPSQMN ISIKDSVLEL RRQRRGMVQT  700
LDQYIFIFKV INDVLTDMGI RSLSSPSKRR SCEMIKSTPM PRLDISIPPP
LTFTPKDFQS SISPSTDMIA SLSIITQMTQ TLKFPPQQQQ DNPFSKSSIK  800
ISPSPLNSTN ISIPKNQQFQ HPFQIQPQLD LNLQQQQQQS SQQLNDNPPL
NMSSNSIKFP PVTSLSSCHL FEDSKNNDNN NKQQQQQQQQ QQKNNQQCSG  900
FSHFLNNNNN NDNNGSSGGG FNGSFLFNSN NSGSSSTNSE CSNNNKNNNN
NSNNNNNNNN NKNSDNNGTK DKDENDSCES PRVTPIKCF
```

FIG. 2. Amino acid sequence derived from *PTP3* cDNA. The catalytic PTP domain is shown in boldface letters, and the conserved catalytic region [consensus, (I/V)HCXAGXGR(S/T)G (52)] is underlined. The three degenerate PCR primers used for *PTP3* isolation hybridized to conserved sequences in the catalytic domain [DYINA for primer 1, DFWRM(I/V)W for primer 2, and HCSAGVGR for primer 3 (see reference 27 for details)].

The catalytic PTP3 domain has 32 to 44% amino acid identity to other PTP domains: 39 and 41% identity to *D. discoideum* PTP1 and PTP2, respectively, 37% identity to human PTP1B (3), and 44% identity to a *Caenorhabditis elegans* PTP identified during the genome sequencing project (64) (GenBank entry July 1995). The sequence alignment shown in Fig. 3 is based upon the known tertiary structure of PTP1B (3). Interestingly, in PTP3 the invariant residues Cys-121 and Trp-125 (numbering of PTP1B) in loop *l*-8 (3) are instead Ala and Tyr, respectively. Also, the highly conserved Met-109 in β-4 and Gly-86 in *l*-4 are in PTP3 Cys and Ala residues, respectively. These unusual, nonconserved amino acids were confirmed by sequencing of genomic DNA. Our data presented below demonstrate that in spite of these departures from conserved residues found in previously characterized PTPs, PTP3 has PTP activity.

PTP3 has phosphatase activity in vitro. A fusion protein between GST and the full-length PTP3 (fused at the first *Eco*RV site [Fig. 1]) could not be detectably expressed in *E. coli* (data not shown), possibly because of its large size (~140 kDa) or because of the stretch of 50 consecutive Asn residues (AAT) in the N-terminal region of PTP3 that could lead to problems with translation when overexpressed in *E. coli*. We were able to successfully express and isolate a truncated ~100-kDa GST-PTP3 fusion protein that lacked these N-terminal sequences but contained the major part of PTP3, including the catalytic domain (construct pMG24; Fig. 1).

The purified GST-PTP3 fusion protein hydrolyzed *p*NPP, a general phosphatase substrate. The hydrolysis rate was found to be proportional to the amount of enzyme used (Fig. 4). The reaction was dependent on the enzyme and the substrate. Vanadate, a PTP inhibitor, inhibited the reaction by 96% at 2 μM. The calculated specific activity for the GST-PTP3 protein was 0.12 $\mu mol\ min^{-1}$ mg of $protein^{-1}$. The recombinant GST-PTP3 was able to dephosphorylate a peptide of $p34^{cdc2}$ [cdc2(6-20)NH_2 (8)] phosphorylated on Tyr with [γ-^{32}P]ATP by the protein tyrosine kinases Src and Lck. This activity was inhibited by 1 μM vanadate (data not shown).

PTP3 is expressed during growth and development. Expres-

```
                     ***                                *   *
PTP1   ETSEGDKKHN TSKNRYTNIL PVNHTRVQLK KIQDKEGSDY INANYIDGAY P...KQFICT QGPLPNTIAD
PTP2   KFRSALEAKN KLKNRYSNVL PFEETRVKI- GDEGTTLSDY INASFINN.. ....GTYICT QGPLLNTIVD
PTP3   KFFSALQPNN YGKNRYHDVL PNESTRVRLT PIESGDG.DY INANYINGEV PNSYRYYIAC QAPLPSTIKD
CEF    TWEHSSADMN KHKNRYANVA AYDHSRVVLS NVEGYPGMDY INANYVDGY. .DKPRSYIAT QGPLPETFSD
PTP1B  PCRVAKLPKN KNRNRYRDVS PFDHSRIKL. ...HQEDNDY INASLIKMEE AQ..RSYILT QGPLPNTCGH
         -----                  --                 -------     --------     ----
         α1                     β1                 β2          β3

       **                    *     *  *  *
PTP1   FWRMVWENRC RIIVMLSRES ENCRIKCDRY WPEQIGGEQF SIYGNGNEVF GTYSVELVEV IQDPEREIIT
PTP2   FWKMIWEQNS NIIVMLTREE ENFKTKCDKY WPDK....DE ERYGNFIVKF DNNITIPDIL IRREFTLEN.
PTP3   FWRMVWEERS SVIVCLTKLE ENGKKKADVY YPET...SQA QEYGSFWIHL HKKVMFKDIG VSSLHLYK..
CEF    FWRMVWEEQS VTIVMLTNLE ERSRVKCDQY WPSR....GT ATYGDIEVTL LESVHLAHYT MRTMRLKM..
PTP1B  FWEMVWEQKS RGVVMLNRVM EKGSLKCAQY WPQKEEKEMI FEDTNLKLTL ISEDIK.SYY TVRQLELEN.
        --------   ----   ---  --                ----    ---     ----   -----------
         α2         β4    β5  β6                β7      β8      β9       β10

                               *  *   *                                 ***** ** *
PTP1   RNIRLTFEGE TRDITQYQYE GWPDHNIPDH TQPFRQLLHS ITNRQNQIIP SSDRNVPIIV HCSAGVGRTG
PTP2   .....LKDNK TRKIYHFQYT TWPDHGTPVS TTGFLKFVSF VDHEK..... ...RSGPIVV HCSAGIGRSG
PTP3   .....KGEEF PREVVLLHYT QWPDCGAPPS SSHIRTLSVM VNTFK.ARGS AKNTNGPVIV HCSAGIGRSG
CEF    .....VGEPE VREIKHLQYT AWPDHGVPDH PTPFLIFLKR VKTLN..... .PNDAGPIIS HCSAGIGRTG
PTP1B  .....LTTQE TREILHFHYT TWPDFGVPES PASFLNFLFK VRES....GS LSPEHGPVVV HCSAGIGRSG
                  ---------             ---------------              -----   -----
                    β11                       α3                      β12

                                            *  *    *   *
PTP1   TFCTAVIM-A IMDKYNSRID ....FNLFSI VLKLREQRPG MVQQLEQYLF CYKTILDEIY
PTP2   TFVAIHSIVA KFAKHYDEKK QAPSINLPKL VVEMRNERPG MVQTRDQYRF CYLAISEAMN
PTP3   TFISININMA KIERFGNDPS QMNIS.IKDS VLELRRQRRG MVQTLDQYIF IFKVINDVLT
CEF    AFIVID.CML ERLRYDN... ...TVDIYGC VTALRAQRSY MVQTEEQYIF IHDAVLDAVN
PTP1B  TFCLADTCLL LMDKRKDPSS ....VDIKKV LLEMRKFRMG LIQTADQLRF SYLAVIEGAK
        --------------              ----------          ----------------
           α4                           α5                  α6
```

FIG. 3. Amino acid sequence comparison of catalytic PTP domains. Shown are the three *D. discoideum* PTPs: PTP1 (GenBank accession no. L07125), PTP2 (GenBank accession no. L15420), and PTP3 (GenBank accession no. U38197); CEF, a *C. elegans* PTP located on cosmid F38A3 (GenBank accession no. Z49938), with a relatively high degree of amino acid identity to PTP3; and human PTP1B (GenBank accession no. M31724). Alignments were performed by hand on the basis of the known tertiary structure data of PTP1B (3) and with the software package of the Genetics Computer Group, Inc. (Madison, Wis.), by using the BESTFIT program to calculate sequence identities. A 99-amino-acid insert in helix α-4 of PTP1 and a 58-amino-acid insert after β-1 in PTP2 are not shown (indicated by dashes). Boldface letters with asterisks represent the invariant amino acids, defined by Barford et al. (3), which were conserved in all 27 catalytically active PTPs investigated. Boldface letters without asterisks represent highly conserved amino acids which were conserved in 24 or more out of 27 PTPs. The conserved catalytic region is boxed.

sion of the PTP3 mRNA was analyzed by RNA blot hybridization (Fig. 5). *PTP3* mRNA was expressed at moderate levels during growth and development. Upon the initiation of development, the *PTP3* transcripts increased by a factor of four and reached a maximum level at 8 h (mound stage). The transcripts then decreased gradually to a level approximately twice that in growing cells.

To identify the cell types expressing *PTP3*, we examined the spatial pattern of expression of stable transformants carrying the PTP3–β-Gal reporter construct (Fig. 1; also see Materials and Methods). The construct used contained ~1.0 kb of 5′ upstream untranscribed sequence similar to the PTP3 overexpression construct (see below and Fig. 1). Two independent clonal isolates that exhibited a relatively high level of β-Gal staining during growth were analyzed further. The cells were starved, plated on filters, and stained histochemically for β-Gal activity at different time points of development (Fig. 6A through F). The results were consistent for both clones. Even though the strains were cloned, only a subset of about 10% log-phase cells showed detectable staining (Fig. 6A). A similar observation has also been made for *PTP2*, *ERK1*, *rasD*, and *Gα1* (11, 15, 18, 27) (see Discussion). At the mound stage (9 h; Fig. 6B), cells staining for PTP3–β-Gal were found scattered throughout the organism. When the first finger had formed (13 h), staining was more concentrated at the base and the tip of

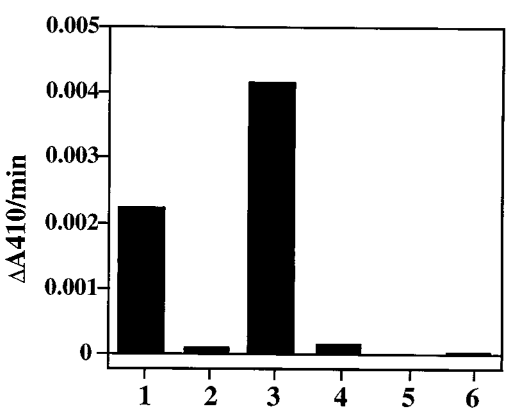

FIG. 4. In vitro assay of phosphatase activity using bacterially purified PTP3. Hydrolysis of *p*NPP was monitored over 116 min as described in Materials and Methods. The six parallel samples had the following variances: bar 1, 1 μg of enzyme; bar 2, 1 μg of enzyme plus 2 μM vanadate; bar 3, 2 μg of enzyme; bar 4, 2 μg of enzyme plus 2 μM vanadate; bar 5, 2 μg of enzyme plus no substrate; and bar 6, substrate plus no enzyme. The height of each column represents the initial slope of the reaction.

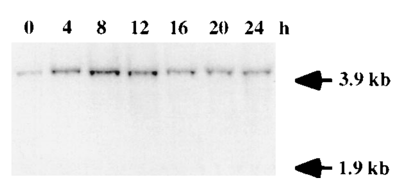

FIG. 5. Developmental Northern blot analysis of *PTP3* mRNA. Six micrograms of total RNA, isolated at 4-h intervals through development, was size fractionated on a denaturing gel, blotted, and hybridized with a PTP3 cDNA probe (the ~500 bp upstream of *Hin*cII; Fig. 1). The changes in relative *PTP3* mRNA levels were quantified by PhosphorImager analysis and were noted as fold increases over vegetative levels: 4 h, 2.7-fold; 8 h, 4.2-fold; 12 h, 3.8-fold; 16 h, 2.4-fold; 20 h, 2.0-fold; and 24 h, 2.5-fold. The arrows point to the positions of the 26S and 17S rRNA bands. UV examination of the RNA blot filter was used to ensure that each lane contained similar levels of rRNA.

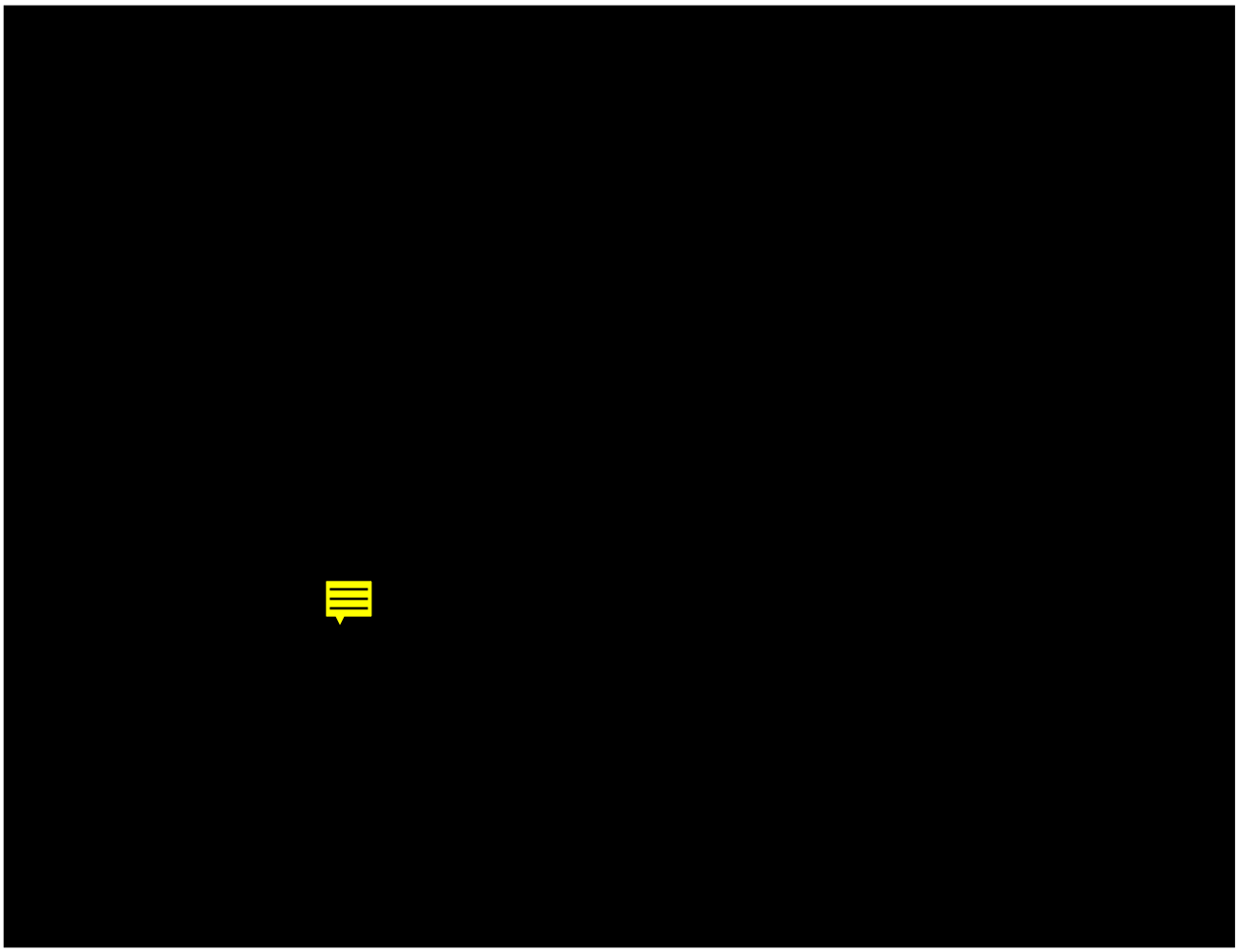

FIG. 6. Spatial expression of *PTP3*. wt cells carrying the PTP3–β-Gal reporter construct (Fig. 1) were plated for development at 7.5×10^5 cells per cm^2. At different time points during development cells were fixed and stained for β-Gal activity driven by the *PTP3* promoter. Two independent clones gave similar results. (A) Vegetative cells (0 h); (B) mound stage (9 h); (C) first finger stage (13 h); (D) slug after 6 h of migration; (E) early culminant stage (21 h); (F) late culminant stage (24 h).

the organism (Fig. 6C). In the slug (17 h), stained cells were observed scattered throughout the organism. As the slug migrated for extended times, the staining was concentrated towards the anterior end (Fig. 6D). During early (21 h [Fig. 6E]) and late (24 h [Fig. 6F]) culminant stages, staining was primarily localized to the lower and upper cups of the differentiating fruiting body as well as to a few cells scattered in the stalk. This expression pattern was similar to that of *PTP2*, during both growth and development (27). During later development (slug and culmination stages), it coincided with the distribution of ALCs and prestalk cells (2, 51, 63). Interestingly, *PTP1* also showed a similar spatial pattern of expression during late development (28).

Gene disruption analysis of *PTP3*. To examine the null phenotype of *PTP3*, we attempted to create a gene disruption by homologous recombination. pMG5 was constructed so that part of the *PTP3* gene was replaced by the *THY1* gene, a prototrophic marker for thymidine. This plasmid was electroporated into the thymidine auxotrophic strain JH10, and stable transformants were selected in thymidine-free medium. Southern blot analysis was performed on 48 thymidine prototrophs obtained in three independent transformations. Each strain showed a band of the size expected for the endogenous gene, indicating that there was at least one remaining copy of the *PTP3* gene. However, 11 of these clonal isolates each had an additional band that was the size expected for the gene disruption fragment. Disruptant and wt bands had equal intensities; no vector sequences were present, and a single copy of *THY1* was integrated into the genome. This result suggested the existence of two copies of *PTP3* in the haploid strain KAx-3 (progenitor strain of JH10 [23]). Extensive Southern blot analysis of the wt strain with eight different restriction endonucleases and three different *PTP3* probes showed only one set of *PTP3*-containing bands, suggesting that the immediate chromosomal environments surrounding the two genomic copies (~15 kb on each side of the PTP3 coding regions) were indistinguishable. Chromosomal mapping with a PTP3 probe as described in reference 34 confirmed the existence of two *PTP3* copies, one on chromosome 1 (*PTPC2*) and one on chromosome 2 (*PTPC1*) (33). Sequencing data from the original PCR products, genomic DNA, and the cDNA clone did not show any deviations, indicating that these cloned fragments originate from one gene or from two apparently identical genes.

Other genes, including those encoding PTP1, are duplicated in the genome (28). In contrast to the results shown here, it was possible to disrupt both *PTP1* genes with *THY1* in a single

transformation (28). To attempt to disrupt the second gene encoding PTP3, the *ptp3* partial knockout strain was transformed with a *PTP3* disruption construct in which the dominant selectable marker conferring resistance against blasticidin S (*bsr*) was used. Southern blot analysis of 12 Bsr^R clonal isolates confirmed the presence of the *bsr* gene. However, in all cases the remaining wild-type *PTP3* gene was intact and in 10 cases the integration of the *PTP3*::*bsr* construct occurred in the region of the previously mutated *PTP3* gene. Reexamination of the original *ptp3* partial-knockout strain exhibited the correct and expected chromosomal configuration. Therefore, the rearrangement happened after the transformation of the *PTP3*::*bsr* knockout construct, presumably by homologous recombination of the new gene disruption construct into this site. The inability to knock out the second gene encoding PTP3 means either that a functional *PTP3* gene is required under our selection conditions or that the second *PTP3* gene is a significantly less efficient target for homologous recombination with the *PTP3*::*bsr* construct (see Discussion).

All 11 *ptp3* partial-knockout strains were analyzed for growth and developmental phenotypes by comparing them with the wt strain KAx-3 or the parental strain JH10. In shaking cultures in axenic medium, the strains grew more slowly (doubling time, 17 ± 4.5 h) than wt cells (doubling time, 11 ± 3.3 h). Large and multinucleated cells were often observed. In contrast, when the cells were grown in association with bacteria on nutrient agar plates, no growth difference between wt and mutant strains was seen. During development, the *ptp3* partial knockout did not show discernible aberrant phenotypes. RNA blot analysis of the *ptp3* partial knockout indicated that PTP3 mRNA was still present, showing that the other *PTP3* gene is expressed (results not shown). Antisense expression has been successfully used to significantly reduce the expression of some (7) but not all (16a) genes with which this technique has been tested. When we expressed *PTP3* antisense transcripts from the discoidin I promoter, which can be repressed by folate during growth (5), no detectable phenotype or detectable reduction in the level of *PTP3* transcripts was found (results not shown), suggesting that the approach did not work for *PTP3.*

Overexpression of wt and mutant PTP3 proteins leads to vegetative and developmental abnormalities. To examine the effect of overexpression of PTP3, plasmid pMG14, which carries the wt full-length *PTP3* gene within 5.1 kb of genomic DNA (Fig. 1), was transformed into strain KAx-3. Clonal isolates from three independent transformations were analyzed for the overexpression of PTP3. Quantitation of Northern blot signals showed that the *PTP3* transcript was overexpressed from 4- to 28-fold. As the *PTP3* mRNA isolated from these strains had the same size as the transcript seen in wt cells, all the *cis* signals for transcription initiation and termination are probably present on the 5.1-kb insert of pMG14.

A detailed analysis of two of the strongly PTP3-overexpressing strains showed that overexpression resulted in lower growth rates in shaking cultures (doubling time, 18 ± 3.2 h). When one clone was kept growing for over a month and then reexamined, the cells had a reduced doubling time of 10 ± 2.3 h, similar to that of a wt strain with an integrated vector conferring $G418^R$ but lacking the *PTP3* gene (pVEII [5]). Western blot analysis showed that the level of PTP3 expression was reduced significantly as the doubling time decreased (Fig. 7A). The cell size for all PTP3 (wt) overexpressors was similar to that of wt cells.

High levels of PTP3 overexpression affected aggregation and the transition phase between early and late development at mound stage. When cells were plated at low densities for development (2.5×10^5 cells per cm^2), very large aggregation streams were observed, in contrast to results with wt cells or strains overexpressing PTP3 to a low level (Fig. 8A and B). The aggregation streams subsequently broke up into small subcenters that resulted in smaller structures than those formed with the strains overexpressing PTP3 to a lesser degree. Up to 50% of the aggregates arrested at the mound stage (Fig. 8D), while the remainder continued with normal kinetics and formed wt-like fruiting bodies.

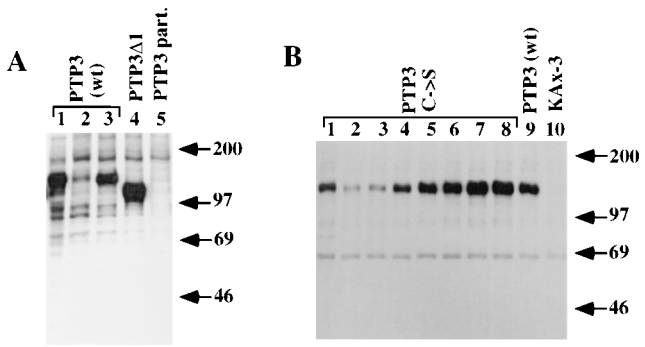

FIG. 7. Anti-PTP3 Western blots of wt and mutant PTP3 overexpressors. (A) The results of vegetative cells overexpressing wt PTP3 at a high level (lanes 1 and 3) or at a low level with a decreased doubling time (lane 2) or overexpressing the internal deletion protein PTP3Δ1 S649 (lane 4) are shown in comparison to the strain carrying a single *PTP3* gene (*ptp3* part., lane 5). As determined by Coomassie staining, the same amount of total protein was loaded for all samples. (B) Clonal analysis by anti-PTP3 Western blotting of different isolates overexpressing PTP3 S649. Protein extracts of eight vegetatively growing isolates (lanes 1 through 8) were compared with those of a strain overexpressing wt PTP3 (lane 9) and to the wt KAx-3 (lane 10). One copy (*ptp3* part. [panel A]) or two copies (KAx-3) of *PTP3* were not enough to give detectable PTP3 levels in Western blots. C→S, Cys-to-Ser mutant. Numbers to the right of each gel are molecular masses (in kilodaltons).

For further functional analysis, the Cys in the active site directly involved in pTyr dephosphorylation (21, 53) was changed to Ser (S649). We made a construct that expressed a GST-PTP3 S649 fusion protein similar to pMG24 (Fig. 1) but which had no phosphatase activity towards *p*NPP (result not shown). In other PTPs that have been examined, the PTP Cys-to-Ser mutant still recognizes its substrate (54) but is unable to hydrolyze the phosphate. This leads to formation of a stable enzyme-substrate complex in vivo, resulting in inhibition of substrate dephosphorylation by the endogenous PTP (38, 41, 55). Plasmid pMG33 encodes the S649 mutation but otherwise is similar to the overexpression construct pMG14 (Fig. 1). Clonal isolates of KAx-3 (pMG33) were screened for overexpression of PTP3 S649 by Western blotting, comparing the protein signal to that seen for wild-type PTP3 (Fig. 7B). Strains identified as having comparably high levels of overexpression of PTP3 S649 had a growth rate (doubling time, 10 ± 3.1 h) that was similar to that of wt cells (see above). However, the cells were considerably smaller than wt and PTP3 (wt) overexpressors and they had an irregular shape, implying an involvement of PTP3 in growth regulation.

As with the overexpression of wt PTP3, overexpression of PTP3 S649 led to large-stream formation during aggregation, at both lower (2.5×10^5 cells per cm^2) and higher (7.5×10^5 cells per cm^2) cell densities (Fig. 8C). These streams broke up into smaller aggregation centers, and very frequently, the original aggregation center produced a large mound that then developed further into a fruiting body that was very much larger than the wt structure (Fig. 8E and F). Considering the smaller size of PTP3 S649-overexpressing cells, a significantly larger number of cells had to be involved in this structure. The

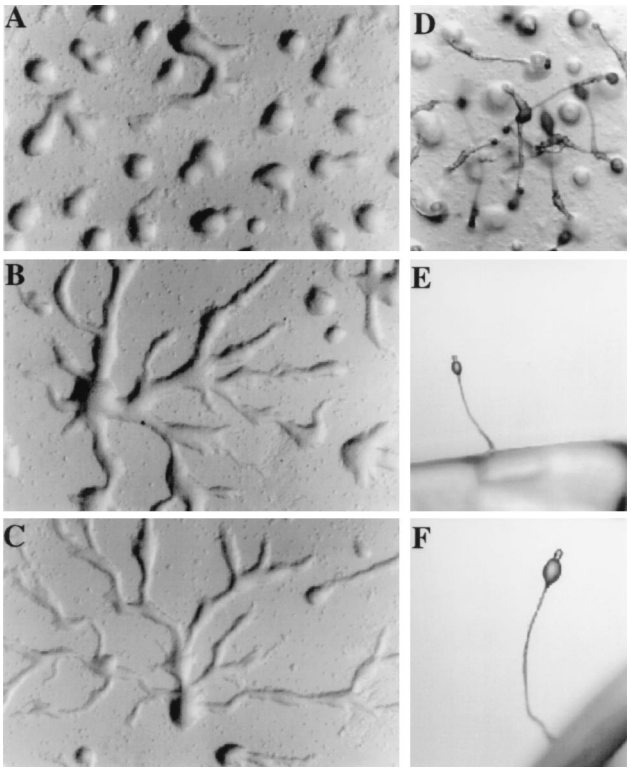

FIG. 8. Developmental phenotypes of KAx-3 cells (A and E) overexpressing wt PTP3 (B and D) or catalytically inactive PTP3 S649 (C and F). Vegetatively growing cells were washed, concentrated in 12 mM sodium-potassium phosphate buffer, pH 6.1, and plated on nonnutrient plates at 2.5×10^5 cells per cm^2. Six hours after the initiation of starvation, KAx-3 cells aggregated to many different centers (A), whereas both overexpressor strains formed large streams pointing to a single center (B and C). All three pictures (A to C) were taken at the same time with the same magnification. Overexpression of wt PTP3 led to an arrest of certain aggregates at the mound stage, and only part of the aggregates developed to the final fruiting-body stage (D). The picture in panel D was taken after 25 h of development and focused on the mounds. The large aggregation center of a PTP3 S649 overexpression mutant developed further to a final structure (F) which was significantly larger than a KAx-3 fruiting body (E) (both pictures were taken with the same magnification).

large slugs often migrated for extended periods of time before culminating, whereas the small aggregates (a variable number between 0 and 50%) either arrested at the mound stage or continued through development with an accelerated timing.

Overexpression of a truncated form of PTP3 (PTP3Δ2 [Fig. 1]) lacking part of the conserved catalytic region, including the consensus sequence (I/V)HCXAGXGR(S/T)G (52), did not show any growth and developmental phenotypes (results not shown).

This diversity of phenotypes of strains overexpressing active and inactive PTP3 suggested that PTP3 might be involved in regulating different steps during development. Most striking was its function in aggregation. Also, the arrest at the mound stage indicated a potential role for PTP3 at the developmental switch between early and late development, the time when major changes in the pattern of pTyr-containing proteins occur (see results below).

Effect of PTP3 mutations on pattern of pTyr-containing proteins. wt cells, *ptp3* partial-knockout cells, and cells overexpressing functional PTP3 or mutant PTP3 S649 were harvested at different times during development and subjected to Western blot analysis with a monoclonal anti-pTyr antibody (Fig. 9; a summary of results is given in Table 1). A number of proteins showed differential tyrosine phosphorylation during development. In wt cells, an increase of Tyr phosphorylation was evident at ~10 h (tipped-aggregate stage) for a 97-kDa protein (doublet) and a 55-kDa protein as described previously (27, 28). These bands remained at the same intensities through the later stages of development. During late culmination (22 and 24 h), two additional proteins became Tyr phosphorylated, one at ~50 kDa and one at 43 kDa, the latter of which we have shown to be actin (29). Other proteins had a constant level of Tyr phosphorylation throughout development.

In the PTP3 (wt) overexpression strain, the doublet protein at 97 kDa showed a higher level of Tyr phosphorylation in vegetative cells (0 h) than in the wt. Upon the initiation of development, these bands decreased in intensity, and at the tipped-aggregate stage only a minor, delayed increase in phosphorylation was observed. Also, the 55-kDa protein showed a smaller increase in tyrosine phosphorylation during the later developmental stages, whereas the phosphorylation of the 50- and 43-kDa proteins was the same as in wt cells. Overexpression of PTP3 S649 also affected the phosphorylation of the doublet at 97 kDa and pp55. As was observed for wt cells, the phosphorylation level of these proteins increased at the tipped-aggregate stage (10 h). However, the phosphorylation was restricted to the slug and culmination stages, and during late culmination (20 h in the experiment shown) it decreased significantly. Again, the phosphorylation of the 50- and 43-kDa proteins was unaffected. Interestingly the *ptp3* partial-knockout strain showed kinetics of p97 and p55 phosphorylation similar to those of the PTP3 S649 overexpressor strain. In contrast to that observed for the other strains, in extracts of the *ptp3* partial-knockout strain, the tyrosine phosphorylation of three proteins with molecular masses between 69 and 200 kDa was elevated at 2 and 4 h.

Major changes in protein tyrosine phosphorylation occur when cells starved in nonnutrient buffer are exposed to growth medium. This shift leads to a transient cell rounding that is accompanied by Tyr phosphorylation of actin (29). PTP1 but not PTP2 is involved in regulating this response (27, 29). In addition to changes in the Tyr phosphorylation of actin (43 kDa) and several other proteins, an ~130-kDa protein (p130) also became transiently phosphorylated under these conditions (Fig. 10A; a summary of results is given in Table 1). Whereas the phosphorylation of this protein was not altered in PTP1 or PTP2 mutants (27, 29), it was drastically reduced in cells overexpressing wt PTP3 (Fig. 10B). In strains overexpressing PTP3 S649 protein, p130 became phosphorylated, following growth medium stimulation, to a lower level than it did in wt cells. Returning the stimulated wt cells to starvation buffer led to a decrease in p130 Tyr phosphorylation; however, p130 remained phosphorylated in PTP3 S649 overexpressors for at least 20 min (Fig. 10C). These results suggested that p130 is a potential substrate of PTP3. In contrast to that of PTP1, the expression level of PTP3 did not affect actin phosphorylation.

Immunoprobing the same protein extracts with anti-PTP3 antibodies revealed a band of 130 kDa (Fig. 7A). To exclude the possibility that PTP3 is pp130, a catalytically inactive PTP3 construct that also carried an internal deletion of 116 amino acids, not including any tyrosines (PTP3Δ1 S649 [Fig. 1]), was made. This protein was overexpressed in KAx-3, and protein extracts were analyzed by Western blotting. The deletion protein migrated at ~110 kDa on SDS gels, which is significantly more rapid than the migration of the full-length PTP3 (Fig. 7A). In growth shift experiments, no new pTyr-containing bands with the mobility of PTP3Δ1 S649 appeared, indicating that the tyrosine-phosphorylated p130 was not PTP3 (Fig. 10D). Similar to cells overexpressing the catalytically inactive

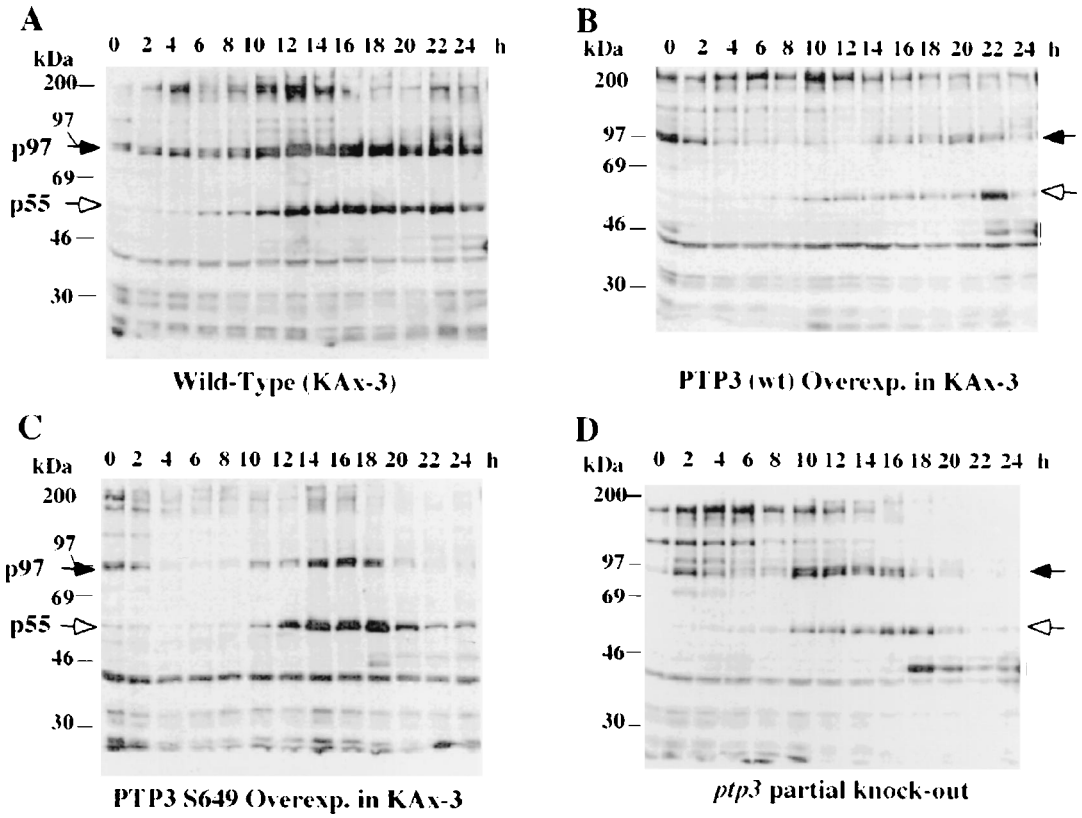

FIG. 9. Developmental time courses of pTyr proteins for the wt (A) and the *ptp3* partial-knockout strain (D) and strains overexpressing wt PTP3 (B) or catalytically inactive PTP3 S649 (C). Exponentially growing cells (4.6×10^7) were starved in 12 mM sodium-potassium phosphate buffer, pH 6.1, and plated for development on 4-cm^2 Millipore filters. At time intervals of 2 h, cells from half a filter were collected and boiled in SDS sample buffer. Equal amounts of protein extracts were separated on SDS gels (8% polyacrylamide) and analyzed by Western blotting using a monoclonal anti-pTyr antibody. The developmental stages were as follows (for KAx-3 [wt], the PTP3 [wt] overexpressor, the PTP3 S649 overexpressor, and the *ptp3* partial knockout, respectively): mound stage, at 8, 12, 8, and 8 h; tipped aggregate stage, at 10, 14, 10, and 10 h; slug stage, at 14, 16, 14, and 12 h; early culminant stage, at 18, 20, 16, and 16 h; and late culminant stage, at 22, 24, 20, and 20 h. These temporal differences do not represent special phenotypes of the investigated strains. As the protein extractions were made on different days they are rather due to variations in the experimental conditions.

full-length PTP3 S649, p130 remained phosphorylated after the shift to buffer. Because the GST-PTP3 fusion protein with the N-terminal truncation (Fig. 1) was still active, it is likely that the deletion in PTP3Δ1 S649 did not affect pp130 recognition. Furthermore, the overexpression of PTP3Δ1 S649 delayed the actin phosphorylation and dephosphorylation by 10 min (Fig. 10D) compared with those of all other strains (Fig. 10A to C).

The *ptp3* partial knockouts did not have any significant detectable effect on the pTyr protein pattern in these growth medium changes (result not shown), although these cells did grow more slowly.

Reversible phosphorylation of PTP3 in response to medium change. When extracts of cells overexpressing wt or mutant PTP3 proteins were blotted and immunoprobed with anti-PTP3 antibodies, it became evident that PTP3 was transiently modified during medium shifts. As illustrated in Fig. 11A, the PTP3Δ1 S649 deletion protein was visible as a doublet band in cells starved for 4 h. After the addition of growth medium, there was a rapid shift of PTP3 protein to a lower mobility. The doublet was replaced by a broad fuzzy band. On a higher-resolution SDS gel, this blurry band consisted of multiple discrete bands (Fig. 11B). After the cells were shifted back to starvation buffer, the mobility of the protein gradually increased, and after 25 min, the lower band of the doublet reappeared (Fig. 11A). As shown in Fig. 11C, this mobility shift was also detected in cells overexpressing full-length wt or mutant PTP3, indicating that PTP3 modification was independent of PTP activity. When anti-PTP3 immunoprecipitates of growth medium-stimulated cells were treated in vitro with the protein Ser-Thr phosphatase PP2A, the PTP3 protein migrated as a doublet band with a mobility similar to that of unstimulated PTP3, indicating that the PTP3 modification was Ser-Thr phosphorylation (Fig. 12). In control reactions, the incubation of growth medium-stimulated immunoprecipitated PTP3 with PP2A in the presence of the PP2A inhibitor microcystin LR or with buffer alone did not lead to more quickly migrating species (Fig. 12). These data further supported an involvement of PTP3 in a growth medium-stimulated response.

DISCUSSION

PTP3, the third PTP identified in *D. discoideum*, lacks any obvious transmembrane sequences, and therefore it is likely to be a nonreceptor PTP (52). Sequence alignment of the catalytic domain with other PTP domains shows amino acid identities similar to those previously determined for PTP1 and PTP2. Interestingly, four highly conserved residues in the catalytic domain, as defined by Barford et al. (3), were not conserved in PTP3. However, on the basis of the crystal structures of PTP1B with and without the substrate analog tungstate (3) or with two peptide substrates (31), these residues would not

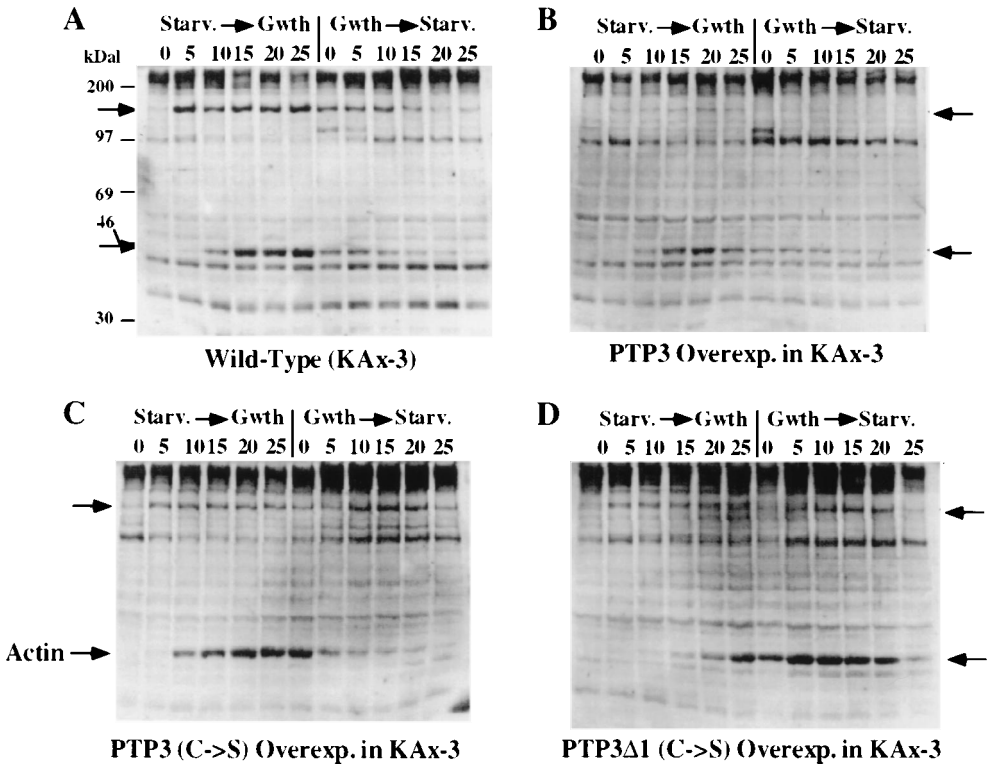

FIG. 10. Changes in the pTyr protein pattern in response to medium stimulation of KAx-3 (A) and PTP3 (wt) (B), PTP3 S649 (C), and PTP3Δ1 S649 (D) overexpressor strains. Exponentially growing cells were washed in 12 mM sodium-potassium phosphate buffer, pH 6.1, and starved in the same buffer while shaking at 150 rpm. After 4 h, the first protein sample was withdrawn and boiled in SDS sample buffer (0 min, Starv.→Gwth), and the rest of the culture was resuspended in growth medium (HL5). Subsequently, samples were taken every 5 min and boiled in SDS sample buffer. After 25 min, the cells were washed and transferred back to sodium-potassium phosphate buffer, and samples were taken in intervals of 5 min for the next 25 min. Equal amounts of proteins were separated on SDS gels (8% polyacrylamide), blotted to membranes, and immunoprobed with anti-pTyr antibody py72.

be directly involved in the catalytic mechanism. Our data showed that PTP3 had phosphatase activity in vitro and that therefore changes to these relatively conserved amino acids were tolerated. In the native PTP1B protein, three of these residues, Met-109, Cys-121, and Trp-125, are located near each other. Possibly the concerted changes to Cys, Ala, and Tyr, respectively, as seen in PTP3, maintain the proper folding and orientation of the amino acid residues within the protein, and the change in only a single amino acid might inhibit enzyme activity. A study of hydroxylamine-mutagenized leukocyte antigen-related PTP domain I showed that replacements with less-conserved amino acids (Gly-1399 to Asp [Gly-86 in PTP1B] or Cys-1434 to Tyr [Cys-121 in PTP1B]) led to complete loss of enzyme activity (60). No known sequence motifs in the large N- and C-terminal regions flanking the catalytic domain of PTP3 were identified. The function of the long homopolymer runs is not known, but these have been seen in a number of *D. discoideum* proteins (see Results).

The specific activity of recombinant GST-PTP3 determined with the substrate *p*NPP was 39 or 13 times lower than the specific activities of bacterially expressed PTP1 (4.66 μmol min^{-1} mg of $protein^{-1}$) or PTP2 (1.57 μmol min^{-1} mg of $protein^{-1}$), respectively (calculated from the results of Howard et al. [28] and Ramalingam et al. [42]). In comparison, GST-pyp3 had a specific activity of ~17.6 μmol min^{-1} mg of $protein^{-1}$ (39) and the dual-specificity phosphatase cdc25 of *Drosophila melanogaster*, isolated from *E. coli*, had an activity of 56 nmol min^{-1} mg of $protein^{-1}$ (12). The relatively low-level activity of PTP3 could be an intrinsic feature of PTP3, possibly due to the unusual amino acids at conserved positions in the catalytic domain (see above). Also, the lack of the N-terminal sequences in the GST fusion protein tested, the lack of necessary activating modifications in the bacterially expressed protein, or the possibility that *p*NPP is an unusually poor substrate for PTP3 could account for the low level of specific activity.

PTP3 was expressed at relatively low levels during growth and development. Disruption of one of the two *PTP3* copies led to slower growth of *D. discoideum* amoebae, which suggests that the mutagenized *PTP3* gene was functional. The presence of PTP3 transcripts in the partial knockout suggests that the remaining gene was also functional. Also, the pTyr-containing-protein pattern during development was altered in the single *ptp3* disruption mutant compared with that of the wt. Interestingly, the *ptp3* partial disruptant showed similarities to the strain overexpressing inactive PTP3 S649 with regard to the phosphorylation kinetics of two proteins (p55 and p97). This result is not unexpected, since both the partial-knockout mutation and the overexpression of the S649 mutation should lead to inefficient dephosphorylation of in vivo substrates for PTP3, albeit for different reasons. No other phenotypes for the *ptp3* partial-knockout strain have been observed.

We were unable to construct a strain with disruptions in both *PTP3* genes, and PTP3 antisense expression was also unsuccessful. The screen for *PTP3* double knockouts was done with two different *PTP3*::*bsr* constructs. The first construct integrated into the already-mutagenized gene (see Results), and the second construct, which had no homology to the *PTP3* gene with the *THY1* disruption (*bsr* cassette inserted into the

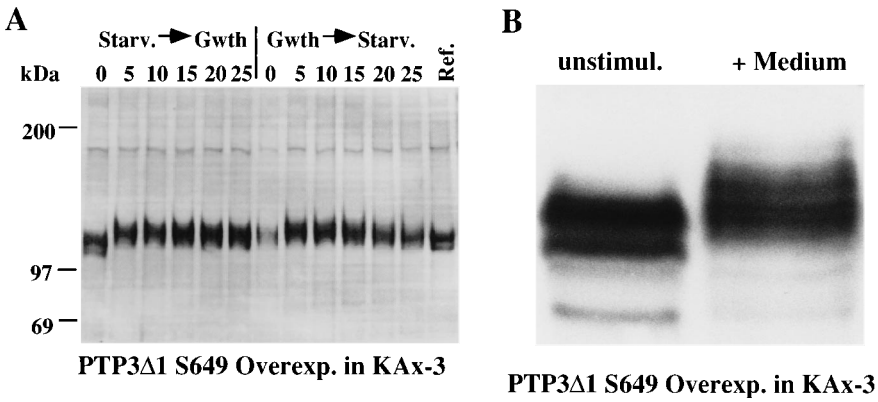

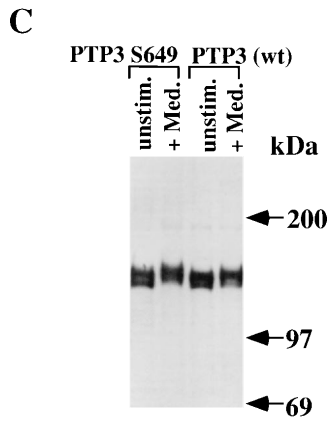

FIG. 11. Posttranslational modification of PTP3 in response to a growth shift. (A) Modification of PTP3Δ1 S649 in response to medium stimulation. The same protein extracts as those shown in Fig. 10D were separated on an SDS gel (6% polyacrylamide) and immunoprobed with polyclonal anti-PTP3 antibody. The first sample (0 min, Starv.→Gwth) was loaded a second time (lane Ref.), after the 25-min Gwth→Starv. time point. (B) Modification of PTP3Δ1 S649 in response to medium stimulation. The same samples as those shown in panel A (cells after 4 h of starvation and after 15 min of medium stimulation) were separated on an SDS gel (10% polyacrylamide gel; 14 by 16 cm^2) and immunoprobed with anti-PTP3 antibody. (C) Modification of full-length PTP3 (wt) and PTP3 S649 in response to medium stimulation. Protein extracts of cells after 4 h of starvation (lanes unstim.) and after the subsequent incubation in growth medium for 15 min (lanes + Med.) were separated on an SDS gel (8% polyacrylamide) and analyzed by Western blotting with anti-PTP3 antibodies.

*Eco*RV-*Pst*I fragment), did not integrate into the second *PTP3* gene (data not shown). There are a number of possibilities to explain these observations: the remaining *PTP3* gene was required for growth under our selection conditions; the second *PTP3* gene was a significantly less efficient target for a homologous recombination; or the second gene lies in a region of the genome that is nonrecombinogenic. It is possible that the same copy of *PTP3* was disrupted in the 11 partial knockouts. Comparison of genomic and cDNA sequencing data did not reveal any differences, presenting the possibility that both sequences might originate from the same gene. However, no differences between the *PTP3* genes at the two loci have been detected by several experimental approaches and it is possible that they are identical. We suggest that both *PTP3* genes are functional and encode the same proteins.

In late development, *PTP3* was expressed in ALCs and prestalk cells. ALCs are scattered throughout the organism and have some molecular properties characteristic of anterior prestalk cells (9, 51). During culmination they sort out and form the upper and the lower cups of the sorus (63). In addition to PTP1 and PTP2, other enzymes involved in signaling pathways, such as Gα4 (23), Gα5 (25), and the mitogen-activated protein kinase ERK1 (18), are expressed in ALCs. Gα4 appears to be involved in a signal transduction pathway leading to the production of a factor required for intercellular signaling (23, 24), supporting the idea that ALCs have a regulatory role within the slug in maintaining the cell type proportioning. Although the three PTPs of *D. discoideum* showed a similar spatial localization pattern, it is not known whether they are expressed in the same subpopulation of ALCs. In addition, it is possible that PTP3 may be expressed at a functional level in other cell types as well.

Overexpression of wt PTP3 led to lower growth rates and streaming during aggregation. The formation of large streams may be caused by fewer cells being able to initiate cAMP signaling. This could be due to a direct involvement of PTP3 in the signal transduction pathway, leading to cAMP pulsing. wt and mutant PTP3-overexpressor strains were checked for their ability to activate ERK2, a mitogen-activated protein kinase required for adenylyl cyclase stimulation (48) (see reference 35 for experimental details). No difference in the kinetics of either activation or inactivation was observed, suggesting that PTP3 is not involved in this part of the pathway (data not shown). In an unsynchronized vegetatively growing cell population, it has been shown that cells starved early in the cell cycle (S and early G_2 phase) were the first to initiate cAMP pulsing (61). Thus, another possible explanation is that PTP3 overexpression might disturb growth regulation by temporally arresting the cell cycle in late G_2 or M phase, so that at any given time, proportionally fewer cells are able to start cAMP pulsing. When expression of the *PTP3-lacZ* reporter was examined during growth phase, only 10% of the cells stained detectably even though clonal strains were examined. This has been observed previously with other genes involved in signaling pathways, including *ERK1*, *rasD*, *PTP2*, and *Gα1* (11, 15, 18, 27). When this was examined further for the *rasD* gene, it was shown that the level of *lacZ* expression changed during the cell cycle, being highest in S and early G_2 (14) (there is no detectable G_1 for *D. discoideum* [62]). It is therefore possible that, like *rasD*, *PTP3* is differentially regulated throughout the cell cycle. If this were the case, it would be consistent with a possible role of PTP3 in regulating the cell cycle and being required for growth. The reduced growth rate caused by overexpression of PTP3 is also consistent with a role of PTP3 in controlling growth regulation.

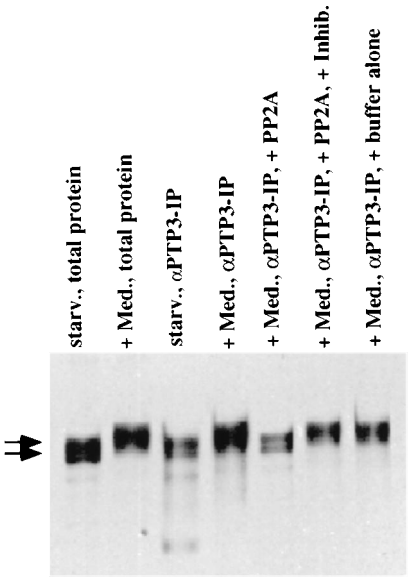

FIG. 12. PTP3 is transiently phosphorylated. wt cells overexpressing the PTP3Δ1 S649 protein were starved in sodium-potassium phosphate buffer. After 2.5 h of incubation, aliquots for total protein analysis and for one immunoprecipitation were withdrawn and subsequently the cells were resuspended in growth medium. Fifteen minutes later, aliquots for total protein analysis and for four immunoprecipitations were taken. The growth medium-stimulated immunoprecipitates were boiled directly in SDS sample buffer, treated with PP2A or PP2A in presence of its inhibitor, microcystin LR, or incubated in phosphatase buffer alone prior to boiling in SDS sample buffer. The immunoprecipitates were then analyzed by anti-PTP3 Western blotting. Arrows point to the doublet band of unstimulated PTPs. For a more detailed description of the experiment see Materials and Methods.

Overexpression of the catalytically inactive PTP3 S649 mutation did not cause the same reduced growth rate observed with overexpression of the wt protein; however, the size of the PTP3 S649-expressing cells was smaller than that of wt cells. It is possible that PTP3 might affect independent pathways, one of which involves growth control and one of which controls aggregation. The arrest at the mound stage caused by the overexpression of both wt and mutant PTP3 proteins may indicate a defect in cAMP signaling. Deletion of the gene encoding cAR2, a prestalk-specific cAMP receptor required for tip formation, also causes a developmental arrest at this stage (44). A repression of cAMP signaling at the mound stage in PTP3 mutants might be expected to exhibit similar phenotypes.

The phenotypes produced by overexpression of wt or mutant proteins need to be evaluated with caution. Greater abundance of a protein can lead to deregulated intracellular localization and to targeting to "false" substrates. However, strains overexpressing PTP1, PTP2, and PTP3 had different growth and developmental phenotypes, indicating that each of these PTPs has different functions and suggesting that at least some of the specificity of these functions is preserved even in the context of overexpression of these proteins. A comparison of the developmental Western blots of these three strains also showed different pTyr-containing-protein patterns even though all three PTPs might be expressed in the same cells. The overexpression of any of these three PTPs did not lead to a general lower content of pTyr proteins. Instead, only the phosphorylation of specific proteins changed. A summary and comparison of the mutant PTP strains based on the observed phenotypes and pTyr patterns are shown in Table 1.

PTP3 S649 was the first mutant protein of this kind expressed in *D. discoideum*. During development, the pattern of pTyr-containing proteins was distinct from that seen with wt cells starting at the culmination stage, although proteins that might be less abundant or not effectively recognized by the py72 anti-pTyr antibody on Western blots might be affected. Other than the larger-sized fruiting bodies that were a consequence of the large aggregation streams, no morphological phenotype could be detected at this time of development.

The stimulation of starved cells by growth medium led to a rapid cell shape change that was correlated with a transient Tyr phosphorylation of specific proteins. This transient Tyr phosphorylation is similar to the intracellular reaction observed after growth factor stimulation of quiescent mammalian cells (30). Our results indicated that PTP3, but not PTP1 (29) or PTP2 (27), strongly affected the dephosphorylation of p130. Moreover, it appeared that p130 is a candidate substrate of PTP3, given that the rate of loss of pp130 tyrosine phosphorylation was specifically reduced in the PTP3 S649 and the PTP3Δ1 S649 mutant strains. Preliminary experiments have shown that the immobilized GST-PTP3 S649 specifically binds pp130 from growth medium-induced cell lysates, which further supports the idea that pp130 is an in vivo PTP3 substrate. It will be interesting to characterize p130 and to find other participants in this pathway.

Concomitant with the Tyr phosphorylation of p130, the growth medium stimulation prompted a quantitative shift of PTP3 to a more slowly migrating species. So far, the known modifications of PTPs are Tyr or Ser-Thr phosphorylations (56), but other mechanisms might also exist. Tyr phosphorylation of PTP3 is unlikely unless it is not detected by the anti-pTyr antibody py72. Treatment of growth medium-stimulated anti-PTP3 immunoprecipitates with PP2A in vitro indicated that PTP3 gets modified by reversible Ser-Thr phosphorylation. Ser and Thr residues are very abundant in PTP3, and it is thus probable from the PP2A experiments that the diffuse PTP3 band was caused by PTP3 being differentially phosphorylated at multiple sites. PTPs can be activated or inactivated through phosphorylation (see References in reference 17). The role of the PTP3 phosphorylation remains to be determined, but it is intriguing to speculate that it may lead to a change in enzyme activity or to a subcellular translocation. These growth shift data strongly imply a function of PTP3 in the signaling pathway(s) leading to cell shape changes. In similar experiments, overexpression of PTP1 led to a lower level of actin Tyr phosphorylation, which correlated with a less-pronounced cell rounding (29). However, no differences in cell shape changes between PTP3 overexpressors and the wt have been seen after medium stimulation. These temporal changes were found to be very difficult to address because cell density, cell size, and the time spent in starvation buffer can vary the cellular reactions drastically (data not shown).

In summary, PTP3 was found to be an enzyme with various roles during *D. discoideum* growth and development. The growth and developmental phenotypes, the distinct pTyr-containing-protein pattern during development and growth shifts, and its modification after medium stimulation demonstrated the specific functions of PTP3 which were clearly different from the functions of the other two PTPs in *D. discoideum.*

ACKNOWLEDGMENTS

We thank members of the Firtel and Hunter laboratories for helpful suggestions, Bill Loomis for mapping and communicating the chromosomal locations of the two *PTP3* genes prior to publication, Christina Allen for carrying out the PCR and the identification of PTP3, Youhang Jiang for screening of the 12- to 16-h λ-ZAP library and the

isolation of cDNA clone 17, Gavin Schnitzler for the use of that library, Joe Dynes for the use of the partial *Sau*3A genomic DNA library, and Peter Kast from the Scripps Research Institute for help with the UV spectrophotometry. We also thank Gernot Walter for providing PP2A enzyme.

M.G. was supported, in part, by a postdoctoral fellowship from the Swiss National Science Foundation. P.H. was supported, in part, by an American Cancer Society postdoctoral fellowship (grant PF-3983). T.H. is an American Cancer Society Research Professor. This work was supported by USPHS grants to T.H. and R.A.F.

REFERENCES

1. **Abe, K., and K. Yanagisawa.** 1983. A new class of rapid developing mutants in *Dictyostelium discoideum*: implications for cyclic AMP metabolism and cell differentiation. Dev. Biol. **95:**200–210.
2. **Abe, T., A. Early, F. Siegert, C. Weijer, and J. Williams.** 1994. Patterns of cell movement within the *Dictyostelium* slug revealed by cell type-specific, surface labeling of living cells. Cell **77:**687–689.
3. **Barford, D., A. J. Flint, and N. K. Tonks.** 1994. Crystal structure of human protein tyrosine phosphatase 1B. Science **263:**1397–1404.
4. **Benson, D. A., M. Boguski, D. J. Lipman, and J. Ostell.** 1996. GenBank. Nucleic Acids Res. **24:**1–5.
5. **Blusch, J., P. Morandini, and W. Nellen.** 1992. Transcriptional regulation by folate: inducible gene expression in *Dictyostelium* transformants during growth and early development. Nucleic Acids Res. **20:**6235–6238.
6. **Burki, E., C. Anjard, J. C. Scholder, and C. D. Reymond.** 1991. Isolation of two genes encoding putative protein kinases regulated during *Dictyostelium discoideum* development. Gene **6:**1–5.
7. **Cao, J.-G., and R. A. Firtel.** 1995. Growth and developmental functions of a human immunodeficiency virus Tat-binding protein/26S protease subunit homolog from *Dictyostelium discoideum*. Mol. Cell. Biol. **15:**1725–1736.
8. **Cheng, H.-C., H. Nishio, O. Hatase, S. Ralph, and J. H. Wang.** 1992. A synthetic peptide derived from p34cdc2 is a specific and efficient substrate of *src*-family tyrosine kinases. J. Biol. Chem. **267:**9248–9256.
9. **Devine, K. M., and W. F. Loomis.** 1985. Molecular characterization of anterior-like cells in *Dictyostelium discoideum*. Dev. Biol. **107:**364–372.
10. **Devreotes, P. N.** 1994. G protein-linked signaling pathways control the developmental program of *Dictyostelium*. Neuron **12:**235–241.
11. **Dharmawardhane, S., A. B. Cubitt, and R. A. Firtel.** 1994. Regulatory role of Gα1 subunit in controlling cellular morphogenesis in *Dictyostelium*. Development **120:**3549–3561.
12. **Dunphy, W. G., and A. Kumagai.** 1991. The cdc25 protein contains an intrinsic phosphatase activity. Cell **67:**189–196.
13. **Dynes, J. L., and R. A. Firtel.** 1989. Molecular complementation of a genetic marker in *Dictyostelium* using a genomic DNA library. Proc. Natl. Acad. Sci. USA **86:**7966–7970.
14. **Esch, K. R.** 1991. Ph.D. thesis. University of California at San Diego, La Jolla.
15. **Esch, K. R., and R. A. Firtel.** 1991. cAMP and cell sorting control the spatial expression of a developmentally essential cell-type-specific *ras* gene in *Dictyostelium*. Genes Dev. **5:**9–21.
16. **Firtel, R. A.** 1995. Integration of signaling information in controlling cell fate decisions in *Dictyostelium*. Genes Dev. **9:**1427–1444.

16a. **Firtel, R. A., et al.** Unpublished observations.

17. **Gamper, M., P. K. Howard, T. Hunter, and R. A. Firtel.** 1995. Protein tyrosine phosphatases in *Dictyostelium discoideum*. Adv. Protein Phosphatases **9:**25–49.
18. **Gaskins, C., M. Maeda, and R. A. Firtel.** 1994. Identification and functional analysis of a developmentally regulated extracellular signal-regulated kinase gene in *Dictyostelium discoideum*. Mol. Cell. Biol. **14:**6996–7012.
19. **Glenney, J. R., Jr., L. Zokas, and M. P. Kamps.** 1988. Monoclonal antibodies to phosphotyrosine. J. Immunol. Methods **109:**277–285.
20. **Guan, K. L., and J. E. Dixon.** 1991. Eukaryotic proteins expressed in *Escherichia coli*: an improved thrombin cleavage and purification procedure of fusion proteins with glutathione S-transferase. Anal. Biochem. **192:**262–267.
21. **Guan, K. L., and J. E. Dixon.** 1991. Evidence for protein-tyrosine-phosphatase catalysis proceeding via a cysteine-phosphate intermediate. J. Biol. Chem. **266:**17026–17030.
22. **Haberstroh, L., and R. A. Firtel.** 1990. A spatial gradient of expression of a cAMP-regulated prespore cell-type-specific gene in *Dictyostelium*. Genes Dev. **4:**596–612.
23. **Hadwiger, J. A., and R. A. Firtel.** 1992. Analysis of Gα4, a G-protein subunit required for multicellular development in *Dictyostelium*. Genes Dev. **6:**38–49.
24. **Hadwiger, J. A., S. Lee, and R. A. Firtel.** 1994. The Gα subunit Gα4 couples to pterin receptors and identifies a signaling pathway that is essential for multicellular development in *Dictyostelium*. Proc. Natl. Acad. Sci. USA **91:**10566–10570.
25. **Hadwiger, J. A., K. Natarajan, and R. A. Firtel.** Mutations in the *Dictyostelium* heterotrimeric G protein α subunit Gα5 alter the kinetics of tip morphogenesis. Development, in press.
26. **Harlow, E., and D. Lane.** 1988. Antibodies: a laboratory manual. Cold Spring Harbor Laboratory, Cold Spring Harbor, N.Y.
27. **Howard, P. K., M. Gamper, T. Hunter, and R. A. Firtel.** 1994. Regulation by protein-tyrosine phosphatase PTP2 is distinct from that by PTP1 during *Dictyostelium* growth and development. Mol. Cell. Biol. **14:**5154–5164.
28. **Howard, P. K., B. M. Sefton, and R. A. Firtel.** 1992. Analysis of a spatially regulated phosphotyrosine phosphatase identifies tyrosine phosphorylation as a key regulatory pathway in *Dictyostelium*. Cell **71:**637–647.
29. **Howard, P. K., B. M. Sefton, and R. A. Firtel.** 1993. Tyrosine phosphorylation of actin in *Dictyostelium* associated with cell-shape changes. Science **259:**241–244.
30. **Hunter, T.** 1995. Protein kinases and phosphatases: the yin and yang of protein phosphorylation and signaling. Cell **80:**225–236.
31. **Jia, Z., D. Barford, A. J. Flint, and N. K. Tonks.** 1995. Structural basis for phosphotyrosine peptide recognition by protein tyrosine phosphatase 1B. Science **268:**1754–1758.
32. **Johnson, R. L., C. L. Saxe III, R. Gollop, A. R. Kimmel, and P. N. Devreotes.** 1993. Identification and targeted gene disruption of cAR3, a cAMP receptor subtype expressed during multicellular stages of *Dictyostelium* development. Genes Dev. **7:**273–282.
33. **Loomis, W. F.** Personal communication.
34. **Loomis, W. F., D. Welker, J. Hughes, D. Maghakian, and A. Kuspa.** 1995. Integrated maps of the chromosomes in *Dictyostelium discoideum*. Genetics **141:**147–157.
35. **Maeda, M., L. Aubry, R. Insall, C. Gaskins, P. N. Devreotes, and R. A. Firtel.** 1996. Seven helix chemoattractant receptors transiently stimulate mitogen-activated protein kinase in *Dictyostelium*. J. Biol. Chem. **271:**3351–3354.
36. **Mann, S. K. O., and R. A. Firtel.** 1987. Cyclic AMP regulation of early gene expression in *Dictyostelium discoideum*: mediation via the cell surface cyclic AMP receptor. Mol. Cell. Biol. **7:**458–469.
37. **Mann, S. K. O., and R. A. Firtel.** 1991. A developmentally regulated, putative serine/threonine protein kinase is essential for development in *Dictyostelium*. Mech. Dev. **35:**89–101.
38. **Milarski, K. L., and A. R. Saltiel.** 1994. Expression of catalytically inactive Syp phosphatase in 3T3 cells blocks stimulation of mitogen-activated protein kinase by insulin. J. Biol. Chem. **269:**21239–21243.
39. **Millar, J. B. A., G. Lenaers, and P. Russell.** 1992. *Pyp3* PTPase acts as a mitotic inducer in fission yeast. EMBO J. **11:**4933–4941.
40. **Nellen, W., and R. A. Firtel.** 1985. High-copy-number transformants and co-transformation in *Dictyostelium*. Gene **39:**155–163.
41. **Noguchi, T., T. Matozaki, K. Horita, Y. Fujioka, and M. Kasuga.** 1994. Role of SH-PTP2, a protein-tyrosine phosphatase with Src homology 2 domains, in insulin-stimulated Ras activation. Mol. Cell. Biol. **14:**6674–6682.
42. **Ramalingam, R., D. R. Shaw, and H. L. Ennis.** 1993. Cloning and functional expression of a *Dictyostelium discoideum* protein tyrosine phosphatase. J. Biol. Chem. **268:**22680–22685.
43. **Sambrook, J., E. F. Fritsch, and T. Maniatis.** 1989. Molecular cloning: a laboratory manual, 2nd ed. Cold Spring Harbor Laboratory, Cold Spring Harbor, N.Y.
44. **Saxe, C. L., III, G. T. Ginsburg, J. M. Louis, R. Johnson, P. N. Devreotes, and A. R. Kimmel.** 1993. CAR2, a prestalk cAMP receptor required for normal tip formation and late development of *Dictyostelium discoideum*. Genes Dev. **7:**262–272.
45. **Schnitzler, G. R., C. Briscoe, J. M. Brown, and R. A. Firtel.** 1995. Serpentine cAMP receptors may act through a G-protein-independent pathway to induce post-aggregative development in *Dictyostelium*. Cell **81:**737–745.
46. **Schnitzler, G. R., W. H. Fischer, and R. A. Firtel.** 1994. Cloning and characterization of the G-box binding factor, an essential component of the developmental switch between early and late development in *Dictyostelium*. Genes Dev. **8:**502–514.
47. **Schweiger, A., O. Mihalache, A. Muhr, and I. Adrian.** 1990. Phosphotyrosine-containing proteins in *Dictyostelium discoideum*. FEBS Lett. **268:**199–202.
48. **Segall, J. E., A. Kuspa, G. Shaulsky, M. Ecke, M. Maeda, C. Gaskins, R. A. Firtel, and W. F. Loomis.** 1995. A MAP kinase necessary for receptor-mediated activation of adenylyl cyclase in *Dictyostelium*. J. Cell Biol. **128:**405–413.
49. **Shaw, D. R., H. Richter, R. Giorda, T. Ohmachi, and H. L. Ennis.** 1989. Nucleotide sequences of *Dictyostelium discoideum* developmentally regulated cDNAs rich in (AAC) imply proteins that contain clusters of asparagine, glutamine, or threonine. Mol. Gen. Genet. **218:**453–459.
50. **Smith, D. B., and K. S. Johnson.** 1988. Single-step purification of polypeptides expressed in *Escherichia coli* as fusions with glutathione *S*-transferase. Gene **67:**31–40.
51. **Sternfeld, J., and C. N. David.** 1982. Fate and regulation of anterior-like cells in *Dictyostelium* slugs. Dev. Biol. **93:**111–118.
52. **Stone, R. L., and J. E. Dixon.** 1994. Protein-tyrosine phosphatases. J. Biol. Chem. **269:**31323–31326.
53. **Streuli, M., N. X. Krueger, A. Y. M. Tsai, and H. Saito.** 1989. A family of receptor-linked protein tyrosine phosphatases in humans and *Drosophila*. Proc. Natl. Acad. Sci. USA **86:**8698–8702.
54. **Stuckey, J. A., H. L. Schubert, E. B. Fauman, Z.-Y. Zhang, J. E. Dixon, and**

M. A. Saper. 1994. Crystal structure of *Yersinia* protein tyrosine phosphatase at 2.5 Å and the complex with tungstate. Nature (London) **370:**571–575.
55. **Sun, H., C. H. Charles, L. F. Lau, and N. K. Tonks.** 1993. MKP-1 (3CH134), an immediate early gene product, is a dual specificity phosphatase that dephosphorylates MAP kinase *in vivo*. Cell **75:**487–493.
56. **Sun, H., and N. K. Tonks.** 1994. The coordinated action of protein tyrosine phosphatases and kinases in cell signaling. Trends Biochem. Sci. **19:**480–485.
57. **Sutoh, K.** 1993. A transformation vector for *Dictyostelium discoideum* with a new selectable marker *bsr*. Plasmid **30:**150–154.
58. **Tan, J. L., and J. A. Spudich.** 1990. Developmentally regulated protein-tyrosine kinase genes in *Dictyostelium discoideum*. Mol. Cell. Biol. **10:**3578–3583.
59. **Tonks, N. K., C. D. Diltz, and E. H. Fischer.** 1988. Characterization of the major protein-tyrosine-phosphatases of human placenta. J. Biol. Chem. **263:**6731–6737.
60. **Tsai, A. Y. M., M. Itoh, M. Streuli, T. Thai, and H. Saito.** 1991. Isolation and characterization of temperature-sensitive and thermostable mutants of the human receptor-like protein tyrosine phosphatase LAR. J. Biol. Chem. **266:**10534–10543.
61. **Wang, M., R. J. Aerts, W. Spek, and P. Schaap.** 1988. Cell cycle phase in *Dictyostelium discoideum* is correlated with the expression of cyclic AMP production, detection, and degradation. Dev. Biol. **125:**410–416.
62. **Weijer, C. J., G. Duschl, and C. N. David.** 1984. A revision of the *Dictyostelium discoideum* cell cycle. J. Cell Sci. **70:**111–131.
63. **Williams, J.** 1995. Morphogenesis in *Dictyostelium*: new twists to a not-so-old tale. Curr. Opin. Genet. Dev. **5:**426–431.
64. **Wilson, R., R. Ainscough, K. Anderson, C. Baynes, M. Berks, J. Bonfield, J. Burton, M. Connell, T. Copsey, J. Cooper, A. Coulson, M. Craxton, S. Dear, Z. Du, R. Durbin, A. Favello, A. Fraser, L. Fulton, A. Gardner, P. Green, T. Hawkins, L. Hillier, M. Jier, L. Johnston, M. Jones, J. Kershaw, J. Kirsten, N. Laisster, P. Latreille, J. Lightning, C. Lloyd, B. Mortimore, M. O'Callaghan, J. Parsons, C. Percy, L. Rifken, A. Roopra, D. Saunders, R. Shownkeen, M. Sims, N. Smaldon, A. Smith, M. Smith, E. Sonnhammer, R. Staden, J. Sulston, J. Thierry-Mieg, K. Thomas, M. Vaudin, K. Vaughan, R. Waterston, A. Watson, L. Weinstock, J. Wilkinson-Sproat, and P. Wohldman.** 1994. 2.2 Mb of contiguous nucleotide sequence from chromosome III of *C. elegans*. Nature (London) **368:**32–38.
65. **Wu, C., M. Whiteway, D. Y. Thomas, and E. Leberer.** 1995. Molecular characterization of Ste20p, a potential mitogen-activated protein or extracellular signal-regulated kinase kinase (MEK) kinase kinase from *Saccharomyces cerevisiae*. J. Biol. Chem. **270:**15984–15992.

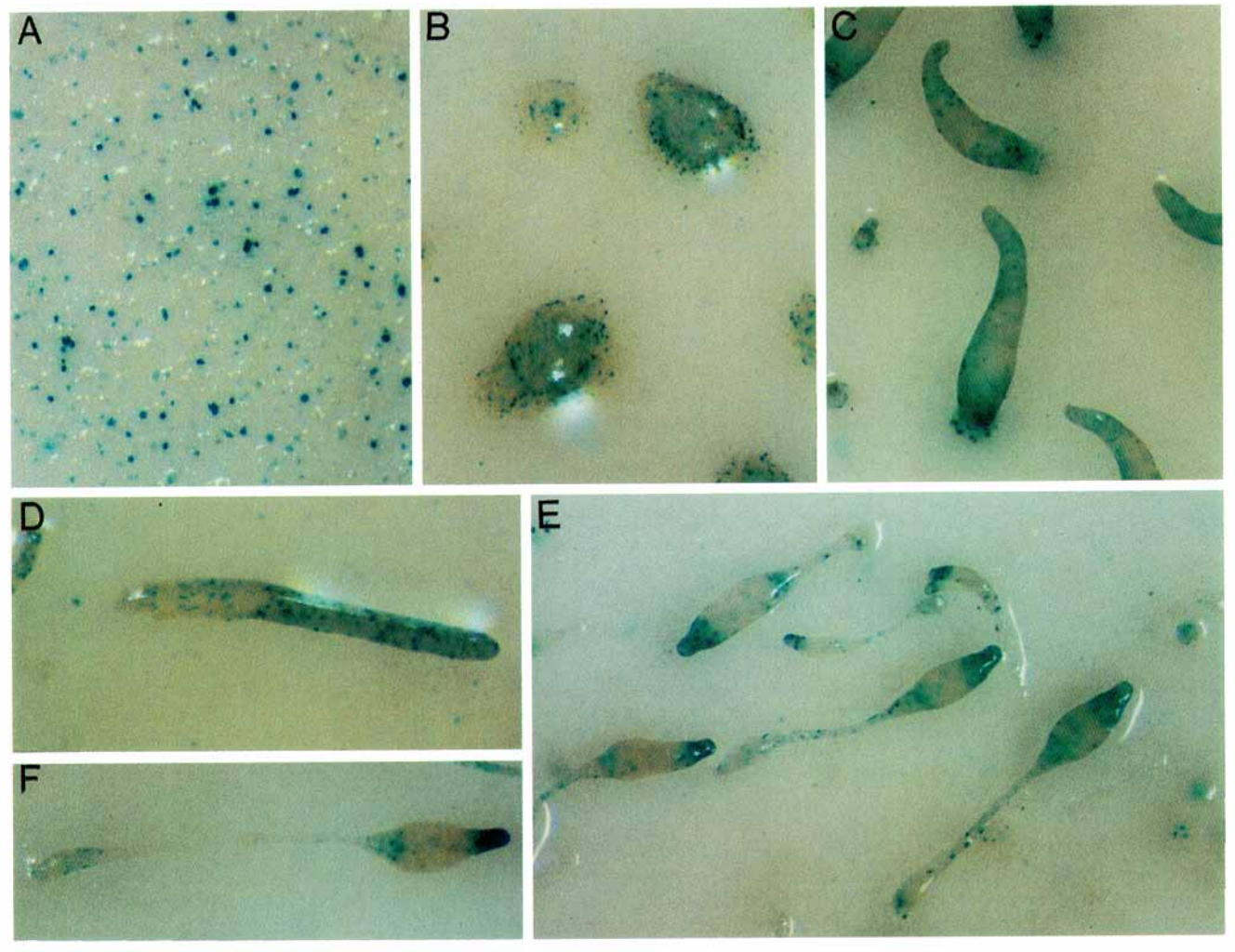
A
B
C
D
E
F